[redacted]

RM A9D25

[redacted]

NACA

RESEARCH MEMORANDUM

AERODYNAMIC STUDY OF A WING-FUSELAGE COMBINATION EMPLOYING A WING SWEPT BACK 63°.- CHARACTERISTICS THROUGHOUT THE SUBSONIC SPEED RANGE WITH THE WING CAMBERED AND TWISTED FOR A UNIFORM LOAD AT A LIFT COEFFICIENT OF 0.25

By J. Lloyd Jones and Fred A. Demele

Ames Aeronautical Laboratory
Moffett Field, Calif.

[redacted]

[redacted]

NATIONAL ADVISORY COMMITTEE
FOR AERONAUTICS

WASHINGTON
August 15, 1949

[redacted]

 [redacted]

NATIONAL ADVISORY COMMITTEE FOR AERONAUTICS

RESEARCH MEMORANDUM

AERODYNAMIC STUDY OF A WING-FUSELAGE COMBINATION EMPLOYING A WING SWEPT BACK 63°.– CHARACTERISTICS THROUGHOUT THE SUBSONIC SPEED RANGE WITH THE WING CAMBERED AND TWISTED FOR A UNIFORM LOAD AT A LIFT COEFFICIENT OF 0.25

By J. Lloyd Jones and Fred A. Demele

SUMMARY

Wind-tunnel tests have been made to determine the independent effects of Mach and Reynolds numbers on the aerodynamic characteristics of a wing-fuselage combination employing a wing having the leading edge swept back 63° and having camber and twist. Tests were also made of the fuselage alone.

Increasing the Mach number from 0.20 to 0.93 resulted in an increase of lift-curve slope from about 0.049 to 0.055 per degree. The abrupt forward movement of the aerodynamic center at the higher lift coefficients, typical of highly swept wings, decreased in severity with increasing Mach number.

The principal effects of increasing Reynolds number from 0.8 million to 9.0 million at a Mach number of 0.20 were a reduction of the drag at positive lift coefficients above about 0.2 and elimination of minor irregularities in longitudinal stability up to a lift coefficient of about 0.55. These data indicate that certain important effects of boundary-layer separation which are evident from tests of highly swept-back wings at low Reynolds numbers may not be present under full-scale conditions.

Characteristics of the wing alone were calculated by subtracting the forces and moments of the fuselage alone from those of the wing-fuselage combination, and no account was made either of wing-fuselage interference or of the wing area enclosed by the fuselage. The characteristics thus obtained are compared with those of a wing of identical plan form but having no camber or twist. The effects of camber and twist were a reduction of the drag at lift coefficients above about 0.1 and an increase of about 33 percent in the lift coefficient at which loss of static longitudinal stability occurred.

[redacted]

INTRODUCTION

The advantages of wings having large amounts of sweepback for efficient flight at supersonic speeds up to Mach numbers of approximately 1.5 have been pointed out by R. T. Jones in reference 1. A coordinated program was formulated for investigation in various facilities of the Ames Aeronautical Laboratory of a wing-fuselage combination designed according to the indications of that study.

Tests to date have shown that the rate of drag increase with lift coefficient was greater than theory predicted, the discrepancy being attributed to boundary-layer separation resulting from an adverse chordwise pressure gradient due to lift, especially severe at the wing tips where the induced upwash is large. Camber and twist have been suggested (reference 1) as possible means of decreasing this adverse pressure gradient. A discussion of the design of a wing incorporating such camber and twist is presented in reference 2, along with the results of tests of this wing at a Mach number of 1.53.

The present report presents the results of tests in the Ames 12-foot pressure wind tunnel of a sting-mounted model of a cambered and twisted wing having the leading edge swept back 63° in combination with a slender fuselage. The model was similar to the model used for the tests reported in reference 2. The effects of the independent variation of Mach and Reynolds numbers on the subsonic characteristics of the wing-fuselage combination and of the fuselage alone are presented. A comparison is made with a wing of identical plan form, but having no camber or twist. Data were obtained at the lowest Reynolds number (0.8 million) to aid in evaluating other data on highly swept wings obtained at comparable Reynolds numbers.

SYMBOLS

The following coefficients and symbols are used in this report:

a speed of sound, feet per second

b wing span measured perpendicular to plane of symmetry, feet

c local chord measured parallel to plane of symmetry, feet

$\bar{c}$ wing mean aerodynamic chord $\left(\dfrac{\int_0^{b/2} c^2 dy}{\int_0^{b/2} c\, dy}\right)$, feet

C_D drag coefficient $\left(\dfrac{\text{drag}}{qS}\right)$

C_L lift coefficient $\left(\frac{\text{lift}}{qS}\right)$

C_m pitching-moment coefficient about the quarter-chord point of the wing M.A.C. $\left(\frac{\text{pitching moment}}{qS\bar{c}}\right)$

$\frac{dC_L}{d\alpha}$ lift-curve slope, per degree

M Mach number $\left(\frac{V}{a}\right)$

q dynamic pressure $\left(\frac{1}{2}\rho V^2\right)$, pounds per square foot

R Reynolds number $\left(\frac{\rho V\bar{c}}{\mu}\right)$

S wing area, square feet

t maximum thickness of wing section, feet

V free-stream velocity, feet per second

y lateral distance, feet

α angle of attack of root chord line, degrees

α_t angle of twist with reference to root chord (positive for washin), degrees

μ coefficient of viscosity of air, slugs per foot-second

ρ mass density of air, slugs per cubic foot

MODEL AND APPARATUS

Photographs of the model used in this investigation are presented in figure 1, and dimensions are given in figures 2 and 3. The wing was constructed of solid steel, and the fuselage of steel and aluminum.

The wing had a leading-edge sweepback of 63°, a tip-chord-to-root-chord ratio of 0.25, and an aspect ratio of 3.5. The streamwise airfoil sections had the NACA 64A005 thickness distribution combined with a=1 mean-camber lines. The wing, as developed theoretically for a lift coefficient of 0.25 at a Mach number of 1.5, was cambered and twisted to support a uniform distribution of lift over its surface. This development was described in reference 2. The model of reference 2 was constructed with less twist than was indicated by theory, the theoretical twist being reduced by the amount expected from wing deflection at the design lift coefficient and at the test dynamic pressure. Since the range of aerodynamic forces encountered in this series of tests was so wide, it was impossible to design the model to compensate for the effects of aerodynamic loading on wing twist. Consequently, the model was designed with the same twist variation under the no-load condition as the model of reference 2. Spanwise variation of camber and twist is shown in figure 3, and section coordinates are given in table I.

The fuselage shape used in this investigation has been determined by Haack (reference 3) to have minimum pressure drag at supersonic speeds for a given length and volume, assuming closure at the tail as indicated by the dashed lines in figure 2. The after 21 percent of the model fuselage length was cut off to permit installation on the sting support. The resultant fineness ratio of the fuselage was 9.9; whereas the fineness ratio of the basic closed body was 12.5. The equation defining the coordinates of the fuselage is given in figure 2.

The model was equipped with constant-chord plain flaps extending over the outer 50 percent of the span. The flap chord was 25 percent of the wing chord at midsemispan. The flap had a radius nose and the unsealed gap was approximately 3/64 inch. This large gap was necessary to permit the desired angular deflection since the flap had considerable spanwise curvature. For the tests reported herein, the flap was undeflected, and was restrained near its inner extremity.

The model was mounted on a sting-type support, and the angle of attack was continuously controllable from a remote station during wind-tunnel operation. All forces and moments were measured by means of a wire-resistance strain-gage balance enclosed by the model.

TESTS

Lift, drag, and pitching-moment data have been obtained throughout an angle-of-attack range for the wing-fuselage combination. The angle-of-attack range for the tests was from -8° to $+19^{\circ}$, except at high Mach numbers and the highest Reynolds numbers where the angle was limited by vibration of either the model or its support, or by wind-tunnel power. At Reynolds numbers of 0.8 million and 2.0 million, data were obtained over a range of Mach numbers up to a maximum of 0.93. At a Mach number of 0.20, data were obtained over a range of Reynolds numbers from 0.8 million to 9.0 million. Lift, drag, and pitching-moment data have been obtained for the fuselage alone throughout the same range of angle of attack and Mach number at a Reynolds number of 2.0 million.

CORRECTIONS

The data have been corrected for the effects of tunnel-wall interference, constriction due to the tunnel walls, base pressure, and static tares due to the weight of the model. No correction has been applied to account for the effect of flap deflection under load upon the force and moment coefficients presented. At the highest loading condition, this deflection was of the order of 1°. The angle of attack of the model was measured visually by means of a cathetometer, hence no corrections were necessary to account for deflection of the support equipment.

Tunnel-Wall Interference

Corrections to the data due to induced tunnel-wall interference have been evaluated by the method of Glauert (reference 4). Since the ratio of model span to tunnel diameter was small, the total corrections were small, and no account was taken of the sweepback of the wing. The following corrections were added:

$$\Delta\alpha = 0.26\ C_L$$

$$\Delta C_L = 0.0046\ {C_L}^2$$

No correction was applied to the pitching moment.

Constriction Effects

The constriction effects of the tunnel walls have been evaluated by the method of reference 5. This method has not been modified to account for the effects of sweepback. The magnitude of the corrections applied to the Mach number and to the dynamic pressure is illustrated by the following table:

Corrected Mach number	Uncorrected Mach number		$\frac{q\text{, corrected}}{q\text{, uncorrected}}$	
	Wing and fuselage	Fuselage alone	Wing and fuselage	Fuselage alone
0.930	0.919	0.921	1.012	1.012
.920	.911	.912	1.010	1.010
.890	.884	.885	1.007	1.007
.850	.846	.847	1.005	1.005
.800	.798	.798	1.003	1.003
.700	.698	.699	1.002	1.002
.600	.599	.599	1.002	1.002
.400	.399	.400	1.001	1.001
.200	.200	.200	1.001	1.001

Base-Pressure Corrections

The pressure on the base of the model fuselage was measured and, in an effort to correct for support interference, the drag data were corrected to correspond to a base pressure equal to the static pressure of the free stream. The effect of longitudinal pressure gradient on drag was calculated and found to be negligible.

Tares

Since the balance was within the model, there were no tares due to direct air forces on the model-support equipment. Corrections were made for the change in static tares due to the weight of the moiel and the variation of model attitude throughout the angle-of-attack range.

PRECISION

The several sources of error affecting the accuracy of the results presented herein are listed below, along with an estimate of their magnitude.

The principal source of error in the data arises from the fact that the precentage accuracy of a given wire-resistance strain gage varies linearly with the absolute magnitude of the force imposed, and that the greatest percentage error occurs with the smallest applied force. The capacities of the gages used were governed by the large variation of forces encountered, and it was not practicable to change gages during the tests to improve the accuracy of the balance. The following table gives an estimate of the precision of the force and moment coefficients as determined from strain-gage calibrations for the limiting values of Mach number and Reynolds number:

M \ R	Wing-fuselage combination			Fuselage alone
	0.8×10^6 (per-cent)	2.0×10^6 (per-cent)	9.0×10^6 (per-cent)	2.0×10^6 (per-cent)
	C_D			
0.20	9	4	1	7
.93	2	1	–	1
	C_L			
.20	1	1	0	4
.93	0	0	–	3
	C_m			
.20	3	1	0	1
.93	0	0	–	0

Calibration of the strain-gage balance indicated that interactions due to deformation of gage members were negligible. Corrections were made for zero shift of the strain indicating instruments.

Another possible source of error in the results was friction in the balance. The effect of friction was largest on the drag measurements of the fuselage alone where the drag force imposed by the weight of the fuselage was large compared to the aerodynamic drag of the fuselage. Reasonably good indication that the effect of frictional forces on the other components was small is the fact that, in general, experimental scatter lies within the limits of error given in the preceding table.

The angle of attack of the model was observed visually by means of a cathetometer. From numerous test readings it was determined that the angle of attack could be set repeatedly within $\pm 0.15^\circ$.

RESULTS AND DISCUSSION

Effects of Mach Number

General aerodynamic characteristics.- General aerodynamic characteristics of the wing-fuselage combination are presented in figures 4 and 5 for Mach numbers from 0.20 to 0.93 and Reynolds numbers of 0.8 million and 2.0 million, respectively. The drag variation with lift (figs. 4(a) and 5(a)) shows no pronounced effect of Mach number. The angle of attack for minimum drag was about 0° throughout the Mach number range. The values of drag coefficient were abnormally low at low lift coefficients for 0.40 Mach number at 0.8 million Reynolds number and for 0.20, 0.40, and 0.70 Mach number at 2.0 million Reynolds number. These small magnitudes are attributed to malfunction of the strain-gage balance rather than to a characteristic of the model.

No pronounced effect of Mach number is noted in the variation of lift coefficient with angle of attack (figs. 4(b) and 5(b)). The angle of attack for zero lift was about 0.5° at a Mach number of 0.20 and increased gradually to about 1.0° at a Mach number of 0.93. A slight decrease in lift-curve slope is noted at a lift coefficient of about 0.2, with subsequent recovery to a value even greater than that at zero lift. Neither the severity of this reduction of slope nor the lift coefficient at which it occurred was affected by Mach number. A corresponding forward movement of the aerodynamic center is discernible from the pitching-moment data (figs. 4(c) and 5(c)) over the range of lift coefficients affected, with subsequent rearward movement to a location generally behind that at zero lift. There was complete loss of static longitudinal stability at the higher lift coefficients. (The lift coefficient at which instability occurred had no consistent variation with Mach number, but was between 0.5 and 0.6 for most of the test Mach numbers.) This trend is typical of the stalling characteristics peculiar to wings with large amounts of sweep (references 6, 7, and 8).

The reduction of lift-curve slope and static longitudinal stability which occurred near a lift coefficient of 0.2 is more apparent than has been observed in other investigations. It is felt that this deviation was due to separation and consequent loss of lift at the wing tips, which, being well back of the moment reference, would have caused a reduction in static longitudinal stability. It is further believed that the rearward movement of the aerodynamic center (subsequent to the forward movement near a lift coefficient of 0.2) resulted from a chordwise redistribution of load, due to separation, wherein the section centers of pressure moved aft. This phenomenon was noted in reference 7. The lift-curve slope increased throughout the range of lift coefficients in which this rearward aerodynamic-center movement occurred, as evidenced by figures 4(b) and 5(b). The abrupt forward movement of the aerodynamic center, beginning at a lift coefficient of about 0.5 to 0.6, probably resulted from wing stall beginning at the tips and progressing inward. Increasing the Mach number reduced the severity of this abrupt forward movement. The pitching-moment coefficient at zero lift was approximately -0.006 and changed very little throughout the Mach number range investigated.

Minimum drag coefficient.- The effect of Mach number on minimum drag coefficient is shown in figure 6 for a Reynolds number of 2.0 million. The minimum drag coefficient increased from about 0.007 to 0.008 for a range of Mach numbers from 0.20 to 0.93. At zero angle of attack (the angle of attack for minimum drag) the outboard sections of the wing were at negative angles, which probably resulted in a greater increase of drag with Mach number than would be the case if all sections were at zero angle of attack.

Lift-curve slope.- The effect of Mach number on lift-curve slope at Reynolds numbers of 0.8 million and 2.0 million is presented in figure 7. Lift-curve slope increased from approximately 0.052 to 0.058 for the test Mach number range at a Reynolds number of 0.8 million and from approximately 0.049 to 0.055 at a Reynolds number of 2.0 million. In all cases, lift-curve slope was measured between lift coefficients of -0.1 and 0.1.

Lift-drag ratio.- The effect of Mach number on lift-drag ratio is presented in figures 8 and 9, which show the variation of lift-drag ratio with lift coefficient for various Mach numbers. The separation at the wing tips, the effects of which have been noted in the lift and moment data at a lift coefficient of about 0.20, is seen to manifest itself as an abrupt termination of the rise of lift-drag ratio with lift coefficient, which occurred at this same lift coefficient (about 0.2). The sharp reduction in lift-drag ratio is a result of the rapid increase of drag which occurred as the lift coefficient was increased above 0.20 or 0.25. A general decrease in maximum lift-drag ratio with increasing Mach number is seen in figure 10. The lift-drag ratios presented are of limited quantitative value however, because of the low degree of accuracy of the drag data at small angles of attack.

The curves presented for 0.4 Mach number at Reynolds numbers of 0.8 million and 2.0 million (figs. 8 and 9) do not correspond to the data of figures 4 and 5. The erroneously low drags obtained at these test conditions, attributed to malfunction of the balance, resulted in corresponding values of lift-drag ratio which were unreasonably high; consequently, the data were retaken. It was later discovered that one flap was deflected slightly during the reruns and the data indicated zero lift at zero angle of attack. The lift-drag ratios presented are from results of the reruns. The erroneous flap angle was very small and it is reasoned that this deflection would not affect the general variation of lift-drag ratio with lift coefficient, although the angle of attack for a given lift-drag ratio would be affected.

Aerodynamic center.- The variation of aerodynamic-center position with Mach number is presented in figure 11. Aerodynamic-center locations were obtained from the linear portions of the moment curves through zero lift; consequently, they are significant only for that limited range. A small rearward movement was noted from approximately 41 to 45 percent of the mean aerodynamic chord as the Mach number increased from 0.20 to 0.93 at Reynolds numbers of 0.8 and 2.0 million.

Effects of Reynolds Number

General aerodynamic characteristics.- General aerodynamic characteristics of the wing-fuselage combination are presented in figure 12 for several Reynolds numbers from 0.8 million to 9.0 million for a Mach number of 0.20. Increasing the Reynolds number reduced the drag at positive lift coefficients above about 0.2 (fig.12(a)). The lift data (fig. 12(b)) indicate that at the higher Reynolds numbers the slight reduction of lift-curve slope due to separation at the tips was reduced in magnitude and delayed to a higher lift coefficient. At a Reynolds number of 9.0 million this reduction began at a lift coefficient of about 0.35. However, the pitching moments at a Reynolds number of 9.0 million (fig. 12(c)) show very little movement of the aerodynamic center from a lift coefficient of -0.1 to a lift coefficient of 0.55, the highest value obtained at this Reynolds number. These data indicate that certain important effects of boundary-layer separation which are evident from tests of highly swept-back wings at low Reynolds may not be present under full-scale conditions.

Minimum drag coefficient.- The variation of minimum drag coefficient with Reynolds number for a Mach number of 0.2 may be seen in figure 6. A gradual increase is noted from approximately 0.007 at a Reynolds number of 2.0 million to 0.010 at 9.0 million.

Lift-curve slope.- Variation of lift-curve slope with Reynolds number is shown in figure 7 for a Mach number of 0.2. The lift-curve slope decreased gradually from 0.051 at a Reynolds number of 0.8 million to 0.046 at 9.0 million.

Lift-drag ratio.- The effect of Reynolds number on lift-drag ratio is presented in figure 13 which shows the variation of lift-drag ratio with lift coefficient at a Mach number of 0.20. It should be noted that at the higher Reynolds numbers (5.0, 7.0, and 9.0 million) the steep drop in lift-drag ratio was delayed to slightly higher lift coefficients, and that, as a result, the lift-drag ratios were near their maximum values over a greater range of lift coefficients.

Attempts were made to obtain an insight on the tip separation at a lift coefficient of 0.2 by employing surface roughness. Full-span roughness strips of 2-percent-chord width were alternately placed at the leading edge of the wing and centered on the 5-percent-chord line. The roughness was achieved by sprinkling carborundum particles (grit No. 180) on an adhesive agent brushed over the desired areas of the wing. The particles covered approximately 80 percent of the area of the strips. The effects of these strips are shown in figure 14. The maximum lift-drag ratio was reduced, probably largely as a result of the increased friction drag due to the increase in the extent of the turbulent boundary layer as a result of fixing transition. However, the alleviation of the premature arrest of the rise of lift-drag ratio with lift coefficient by use of the roughness at the leading edge would seem to indicate that the boundary layer separating at the tip was laminar.

Variation of maximum lift-drag ratio with Reynolds number is presented in figure 10. A decrease occurred from approximately 15.8 at 2.0 million Reynolds number to approximately 14.5 at 6.5 million with a subsequent increase to 15.2 at 9.0 million.

Aerodynamic center.- The variation of aerodynamic-center location with Reynolds number is presented in figure 11. A slight and nearly linear forward movement of the aerodynamic center is noted from 41 percent of the mean aerodynamic chord at 0.8 million Reynolds number to 39 percent at 9.0 million.

Aerodynamic Characteristics of the Fuselage

Aerodynamic characteristics of the fuselage are presented in figure 15 for several Mach numbers for a Reynolds number of 2.0 million. Evidence of the effect of friction in the balance is noted in the discontinuous character of the drag data near zero angle of attack for the lower values of Mach number. Friction, which acted in opposite directions for positive and negative angles of attack, accounts for the asymmetry of the curves of drag-coefficient variation with angle of attack.

Effects of Camber and Twist

General aerodynamic characteristics.- Characteristics of the wing alone are compared in figure 16 with those of a wing of identical plan form, but having no camber or twist (reference 9). It must be noted that the wing of reference 9 was tested as a semispan model mounted from the tunnel wall and that the gap at the root chord and the existence of a boundary layer on the tunnel wall would have the effect of reducing the effective aspect ratio. That this effect was small is evidenced by the close agreement between the results of the tests of the semispan model (reference 9) and the results of tests of a complete model of a similar wing (reference 8). Furthermore, the cambered and twisted wing of this investigation had streamwise sections of 5-percent-chord thickness as compared with 6-percent-chord thickness for the sections of the plane wing discussed in reference 9. Wing-alone characteristics for the cambered and twisted wing were calculated by subtracting the data obtained from tests of the fuselage from those obtained from tests of the wing-fuselage combination. No account was taken of wing-fuselage interference.

A comparison is made in figure 16 of the aerodynamic characteristics of the two wings at several Mach numbers for Reynolds numbers of approximately 2 million. The principal effect of camber and twist upon the drag characteristics was a reduction of drag at positive lift coefficients above a lift coefficient of about 0.1, indicating an increase in maximum lift-drag ratio. The lift data (fig. 16(b)) indicate a slightly more pronounced reduction of lift-curve slope due to separation at the tips at a lift coefficient of about 0.2 for the cambered and twisted wing. This reduction of lift-curve slope for the cambered and twisted wing occurred at a slightly higher lift coefficient than for the plane wing of reference 9. This delay was probably the result of the reduced angle of attack of the tips due to wing twist. The angle of attack for zero lift was about 0.5° for the cambered and twisted wing as compared with 0° for the plane wing.

Figure 16(c) shows an increase in static longitudinal stability due to camber and twist. The forward movement of the aerodynamic center at a lift coefficient of approximately 0.2, due to separation at the tips, was, in general, slightly more pronounced for the cambered and twisted wing, and occurred at a higher lift coefficient. The final deterioration of stability of the cambered and twisted wing occurred at a lift coefficient about 0.15 higher (approximately 33 percent) than for the plane wing. The cambered and twisted wing had a moment coefficient at zero lift of approximately -0.01; whereas the plane wing of reference 9 had no pitching moment at zero lift.

CONCLUDING REMARKS

The results of tests of the cambered and twisted wing with the leading edge swept back 63° in combination with a slender fuselage indicate the following:

Effects of Mach Number

There was little difference in Mach number effects on the wing-fuselage combination for Reynolds numbers of 0.8 million and 2.0 million. Variation of Mach number from 0.20 to 0.93 at a Reynolds number of 2.0 million affected the aerodynamic characteristics as follows:

1. The abrupt forward movement of the aerodynamic center beginning at a lift coefficient of about 0.5 to 0.6 was reduced in severity.

2. The aerodynamic center at zero lift moved rearward from about 41 percent of the mean aerodynamic chord to about 45 percent.

3. The lift-curve slope increased from about 0.049 to 0.055 per degree.

Effects of Reynolds Number

Increasing Reynolds number from 0.8 million to 9.0 million at a Mach number of 0.20 affected the aerodynamic characteristics of the wing-fuselage combination as follows:

1. Minor irregularities in static longitudinal stability were virtually eliminated up to a lift coefficient of about 0.55.

2. The drag was reduced at positive lift coefficients above a lift coefficient of about 0.2.

3. The lift-curve slope decreased from 0.051 to 0.046 per degree.

4. The aerodynamic-center position at zero lift was little affected by changes in Reynolds number, moving from 41 percent to 39 percent of the mean aerodynamic chord.

5. The data from these tests indicate that certain important effects of boundary-layer separation which are evident from tests of highly swept-back wings at low Reynolds numbers may not be present under full-scale conditions.

Effects of Camber and Twist

The following effects of camber and twist were indicated by a comparison of the results for the cambered and twisted wing with those for a wing of identical plan form having no camber or twist:

1. The drag coefficients were reduced at positive lift coefficients above about 0.1.

2. The abrupt forward movement of the aerodynamic center was delayed to a lift coefficient about 0.15 higher, an increase of approximately 33 percent.

3. The angle of attack for zero lift was about 0.5° as compared to 0° for the wing with no camber or twist.

Ames Aeronautical Laboratory,
National Advisory Committee for Aeronautics,
Moffett Field, Calif.

REFERENCES

1. Jones, Robert T.: Estimated Lift-Drag Ratios at Supersonic Speed. NACA TN 1350, 1947.

2. Madden, Robert T.: Aerodynamic Study of a Wing-Fuselage Combination Employing a Wing Swept Back 63°.– Investigation at a Mach Number of 1.53 to Determine the Effects of Cambering and Twisting the Wing for Uniform Load at a Lift Coefficient of 0.25. NACA RM A9C07, 1949.

3. Haack, W.: Geschossformen Kleinsten Wellenwiderstandes. Lilienthal-Gesselschaft für Luftfahrtforschung. Bericht 139, Teil 1, 1946, pp. 14-28.

4. Glauert, H.: Wind-Tunnel Interference on Wings, Bodies and Airscrews. R. & M. 1566, 1933.

5. Herriot, John G.: Blockage Corrections for Three-Dimensional-Flow Closed-Throat Wind Tunnels, with Consideration of the Effect of Compressibility. NACA RM A7B28, 1947.

6. Soulé, Hartley A.: Influence of Large Amounts of Wing Sweep on Stability and Control Problems of Aircraft. NACA TN 1088, 1946.

7. McCormack, Gerald M., and Cook, Woodrow L.: A Study of Stall Phenomena on a 45° Swept-Forward Wing. NACA TN 1797, 1949.

8. McCormack, Gerald M., and Walling, Walter C.: Aerodynamic Study of a Wing-Fuselage Combination Employing a Wing Swept Back 63°.– Investigation of a Large-Scale Model at Low Speed. NACA RM A8D02, 1949.

9. Reynolds, Robert M., and Smith, Donald W.: Aerodynamic Study of a Wing-Fuselage Combination Employing a Wing Swept Back 63°.– Subsonic Mach and Reynolds Number Effects on the Characteristics of the Wing and on the Effectiveness of an Elevon. NACA RM A8D20, 1948.

CONFIDENTIAL

TABLE I.– AIRFOIL SECTION COORDINATES

[All values given in percent chord]

c_0			
Lower surface		Upper surface	
Station	Ordinate	Station	Ordinate
0	0	0	0
.5	–.404	.5	.404
.75	–.488	.75	.488
1.25	–.616	1.25	.616
2.50	–.847	2.50	.847
5.00	–1.166	5.00	1.166
10.0	–1.599	10.0	1.599
20.0	–2.131	20.0	2.131
30.0	–2.413	30.0	2.413
40.0	–2.499	40.0	2.499
50.0	–2.354	50.0	2.354
60.0	–2.032	60.0	2.032
70.0	–1.589	70.0	1.589
80.0	–1.071	80.0	1.071
90.0	–.541	90.0	.541
100.0	–.011	100.0	.011

c_1			
Lower surface		Upper surface	
Station	Ordinate	Station	Ordinate
0	0	0	0
.526	–.366	.474	.438
.778	–.433	.726	.536
1.283	–.536	1.221	.690
2.535	–.706	2.463	.984
5.039	–.927	4.956	1.401
10.041	–1.211	9.959	1.984
20.036	–1.530	19.964	2.725
30.026	–1.685	29.974	3.138
40.010	–1.700	39.990	3.297
50.00	–1.530	50.000	3.179
59.990	–1.231	60.010	2.828
69.985	–.860	70.015	2.313
79.985	–.479	80.015	1.669
89.985	–.155	90.015	.927
100.000	– – –	100.000	– – –

c_2			
Lower surface		Upper surface	
Station	Ordinate	Station	Ordinate
0	0	0	0
.532	–.357	.469	.457
.788	–.419	.713	.557
1.295	–.507	1.208	.720
2.547	–.663	2.447	1.026
5.056	–.851	4.944	1.477
10.056	–1.089	9.944	2.103
20.044	–1.345	19.956	2.912
30.031	–1.458	29.969	3.373
40.013	–1.446	39.987	3.548
50.000	–1.270	50.000	3.436
59.987	–.982	60.013	3.085
69.981	–.632	70.019	2.547
79.975	–.288	80.025	1.852
89.981	–.031	90.019	1.045
100.000	– – –	100.000	– – –

c_3			
Lower surface		Upper surface	
Station	Ordinate	Station	Ordinate
0.533	–0.350	0.470	0.462
.788	–.414	.709	.557
1.298	–.502	1.202	.725
2.556	–.645	2.444	1.043
5.056	–.828	4.944	1.497
10.056	–1.051	9.944	2.150
20.048	–1.290	19.952	2.978
30.032	–1.377	29.968	3.447
40.016	–1.361	39.984	3.639
50.000	–1.186	50.000	3.527
59.984	–.892	60.016	3.169
69.976	–.557	70.024	2.627
79.976	–.223	80.024	1.911
89.984	.008	90.016	1.091
100.000	– – –	100.000	– – –

c_4			
Lower surface		Upper surface	
Station	Ordinate	Station	Ordinate
0.536	–0.350	0.470	0.460
.799	–.405	.711	.558
1.291	–.503	1.204	.722
2.549	–.646	2.440	1.039
5.055	–.832	4.945	1.489
10.055	–1.050	9.945	2.144
20.044	–1.291	19.956	2.976
30.033	–1.389	29.967	3.425
40.022	–1.368	39.978	3.621
50.000	–1.193	50.000	3.512
59.989	–.908	60.011	3.162
69.978	–.569	70.022	2.604
79.978	–.230	80.022	1.915
89.978	.011	90.022	1.083
100.000	– – –	100.000	– – –

c_5			
Lower surface		Upper surface	
Station	Ordinate	Station	Ordinate
0.543	–0.350	0.473	0.455
.788	–.420	.718	.560
1.278	–.508	1.208	.718
2.557	–.648	2.452	1.033
5.061	–.823	4.956	1.494
10.070	–1.068	9.965	2.119
20.053	–1.313	19.947	2.960
30.035	–1.419	29.965	3.415
40.018	–1.401	39.982	2.608
50.000	–1.208	50.000	3.485
59.982	–.928	60.018	3.135
69.982	–.595	70.018	2.592
79.982	–.245	80.018	1.891
89.982	–.018	90.018	1.068
100.000	– – –	100.000	– – –

Note: Spanwise positions of airfoil sections c_0 to c_5 are shown in figure 3.
For all sections: Leading-edge radius = 0.175. Trailing-edge radius = 0.014.

NACA

CONFIDENTIAL

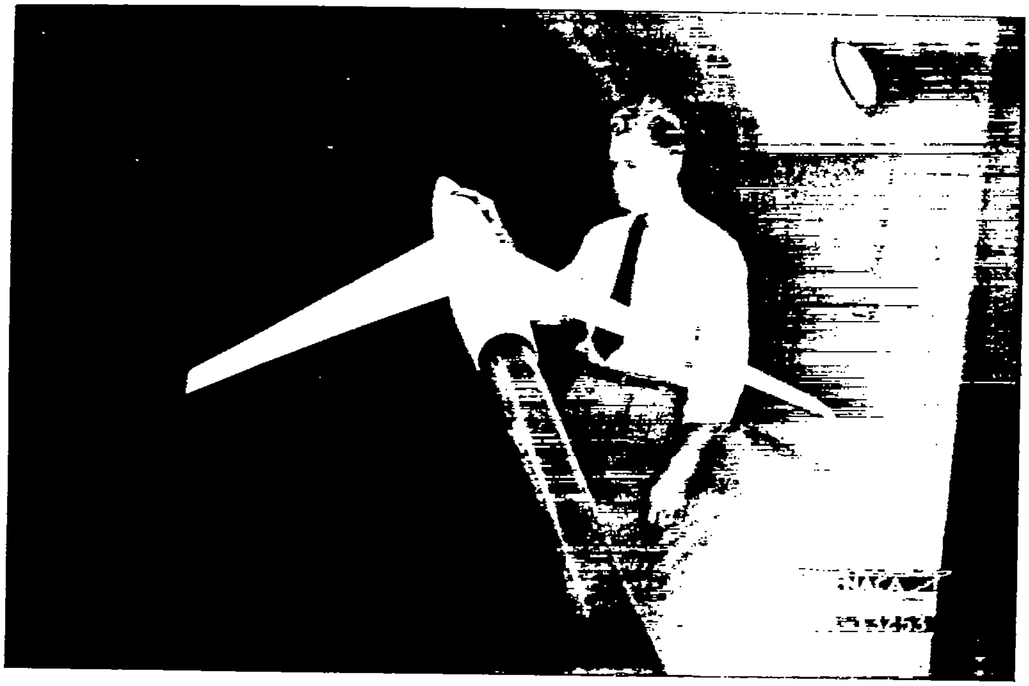

(a) Rear view.

(b) Plan view.

Figure 1.– Model of the cambered and twisted wing with the leading edge swept back 63° in combination with a fuselage.

[redacted]

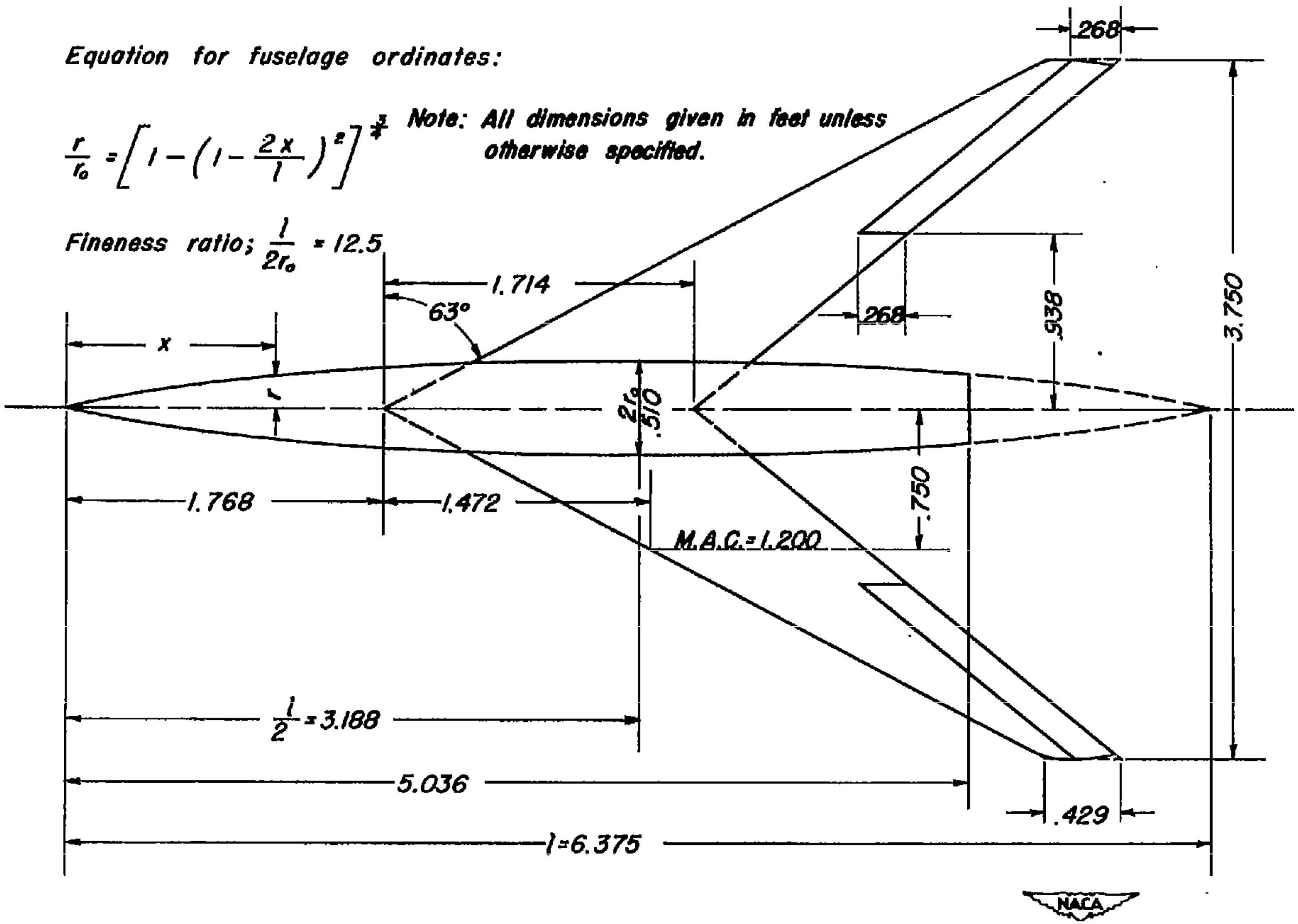

Figure 2.— Dimensions of wing and fuselage.

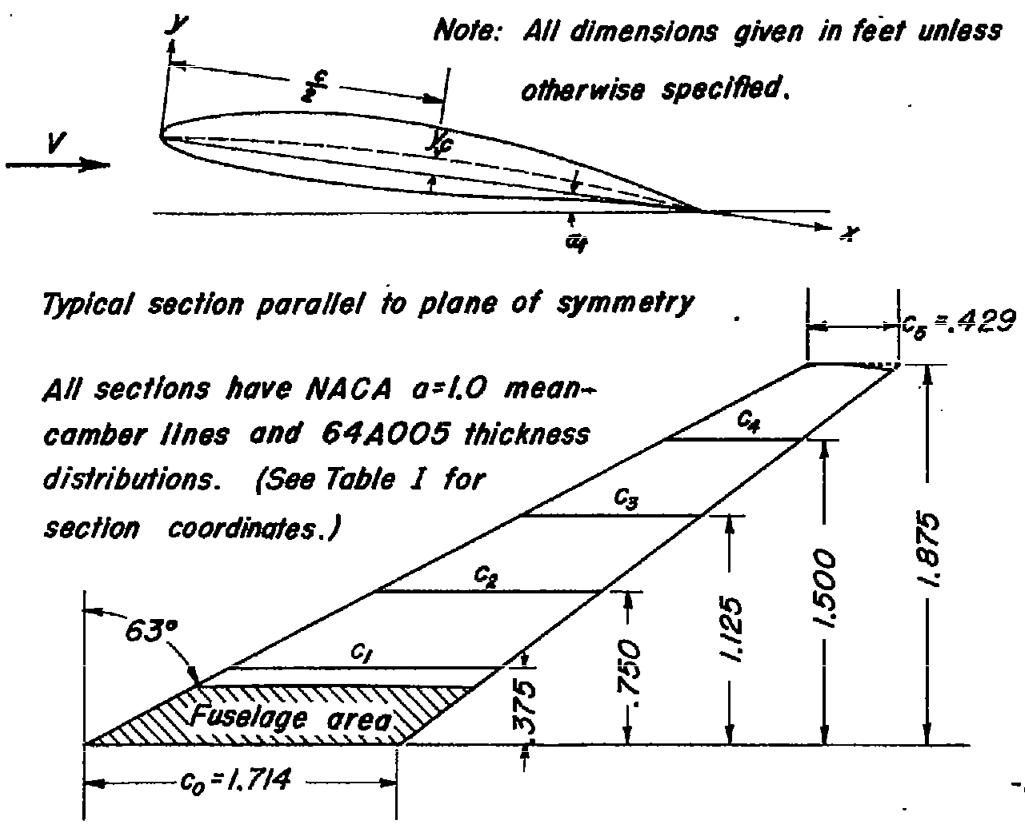

Spanwise camber distribution

Station	Percent semi-span	Camber y_c/c
c_0	0	0
c_1	20	.0082
c_2	40	.0108
c_3	60	.0117
c_4	80	.0115
c_5	100	.0114

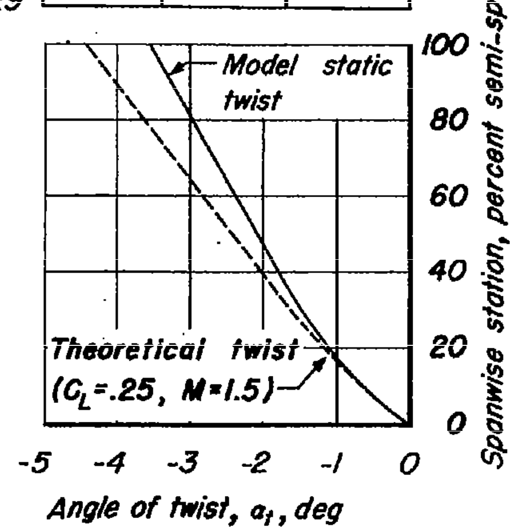

NACA

Figure 3.— Plan form of right half of wing showing spanwise variation of camber and twist and location of sections for which coordinates have been calculated.

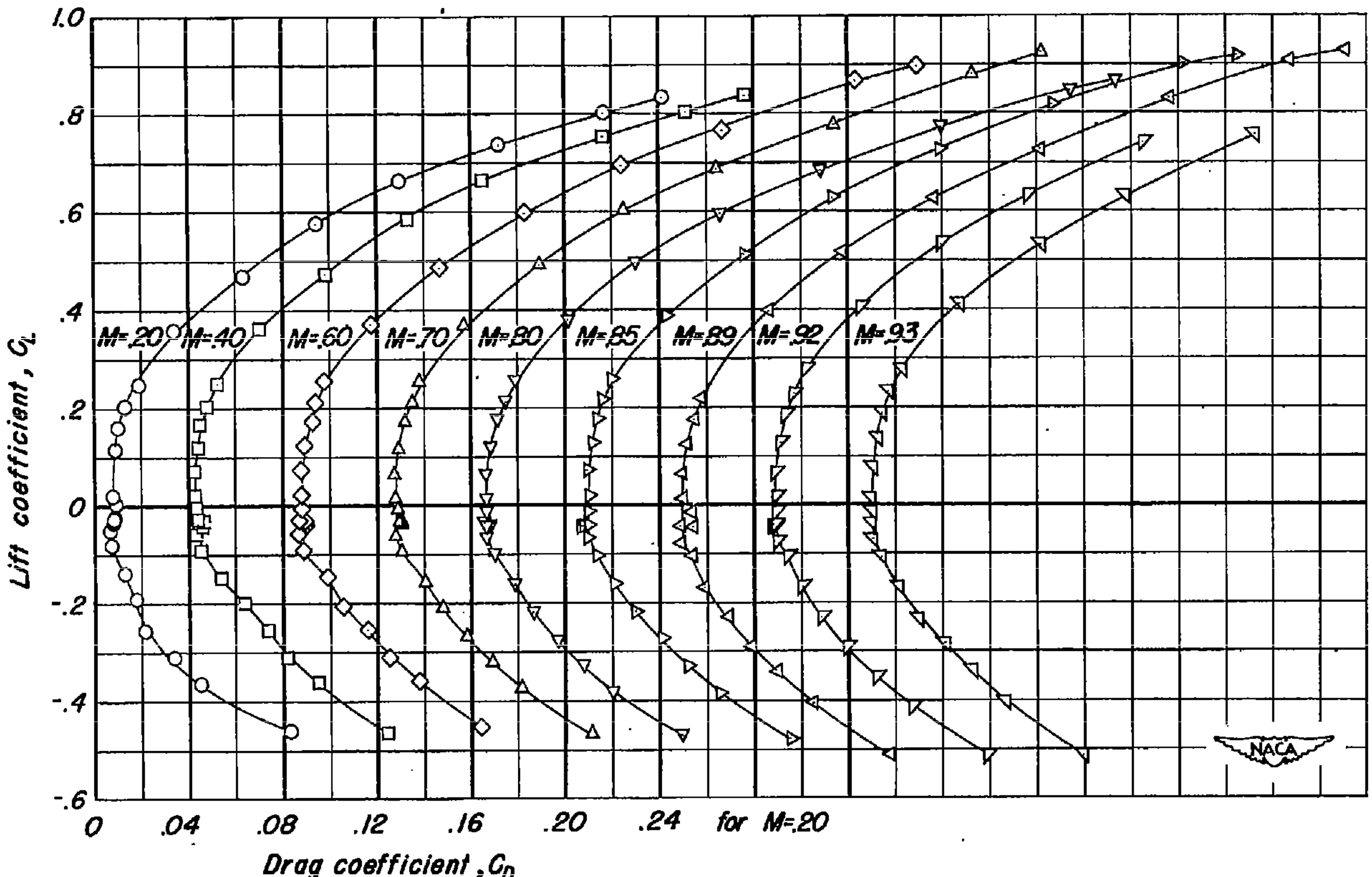

(a) C_L vs C_D.

Figure 4.– The effect of Mach number on the aerodynamic characteristics of the wing-fuselage combination at a Reynolds number of 800,000.

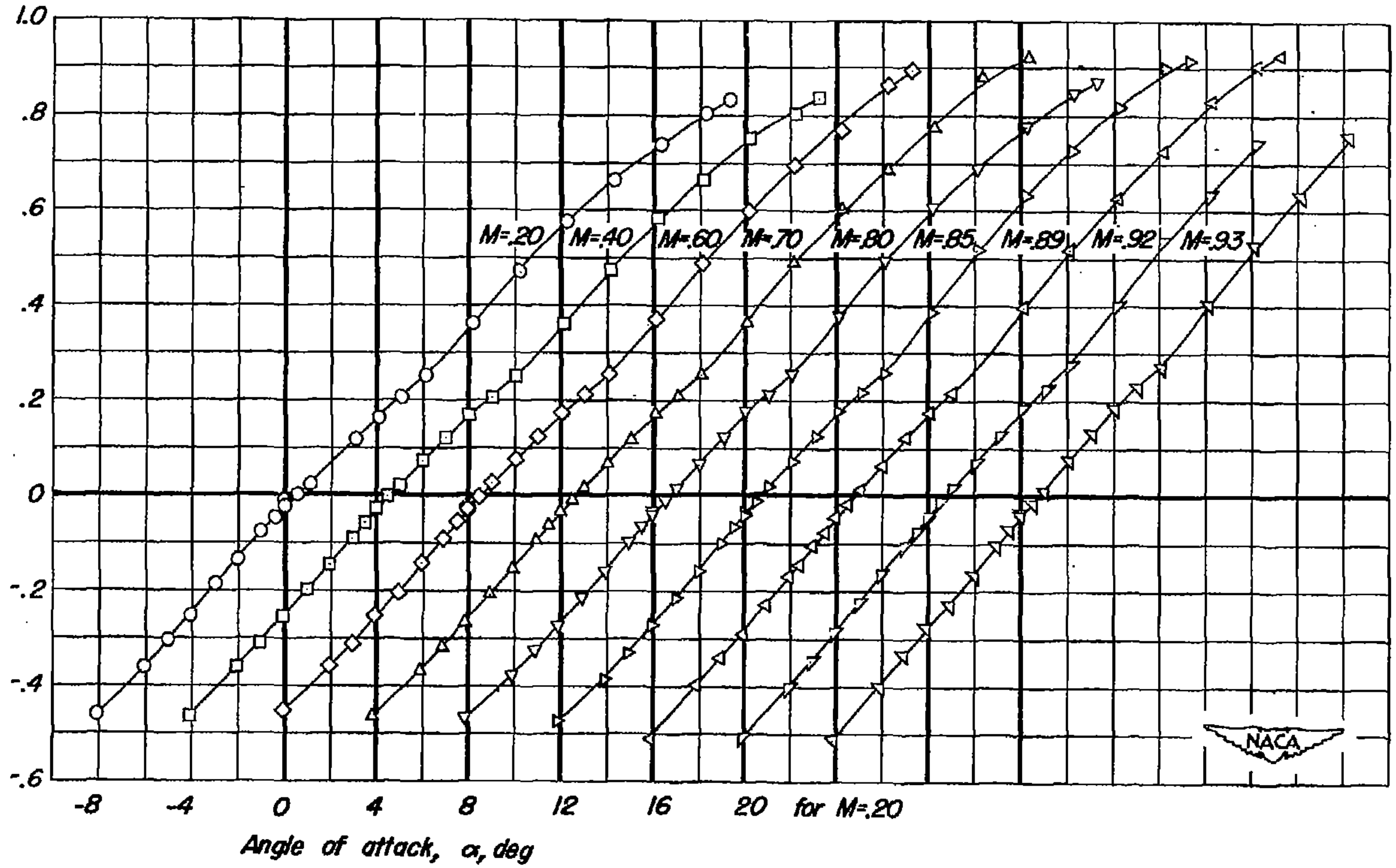

(b) C_L vs α.

Figure 4.- Continued.

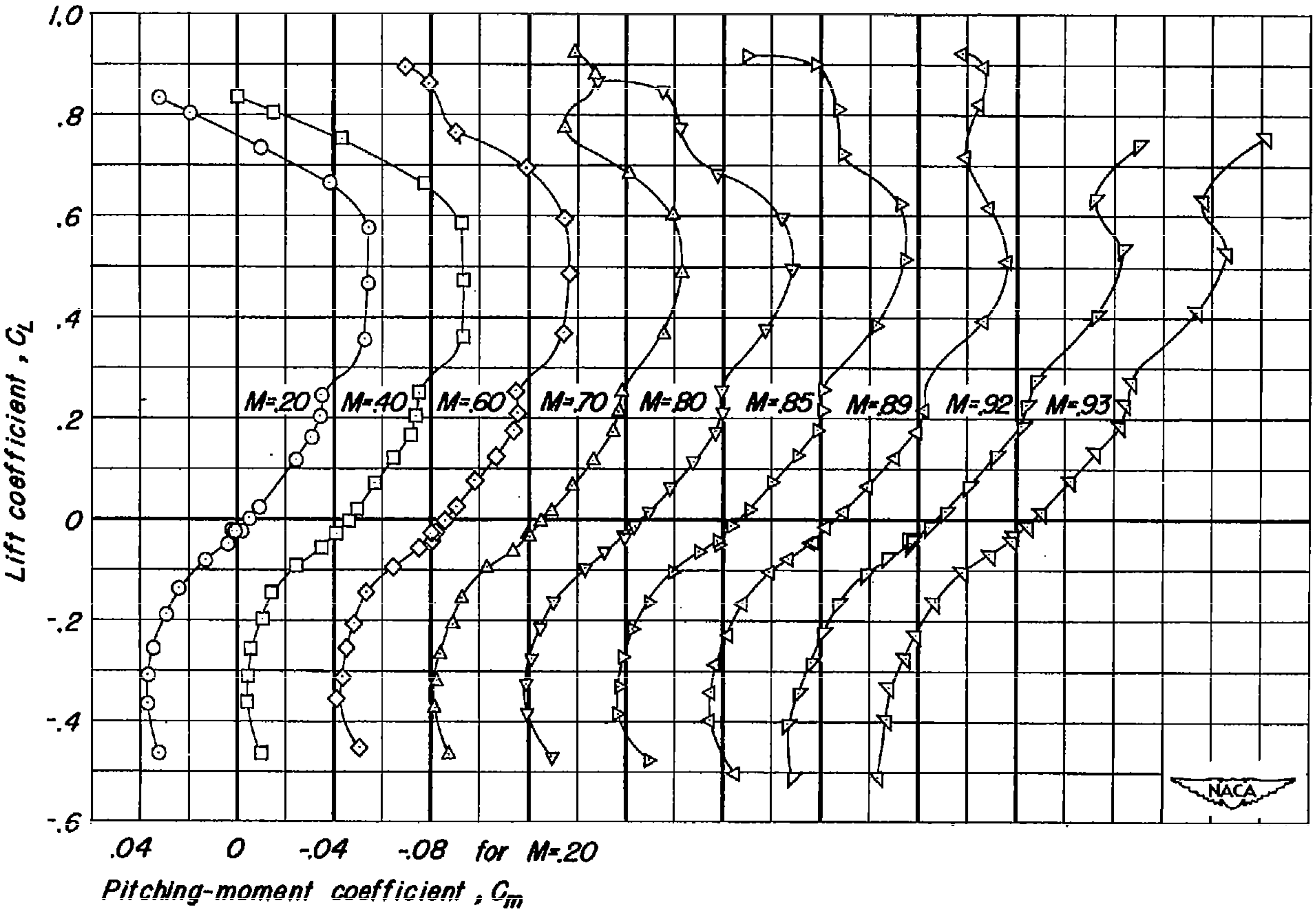

(c) C_L vs C_m .

Figure 4.– Concluded.

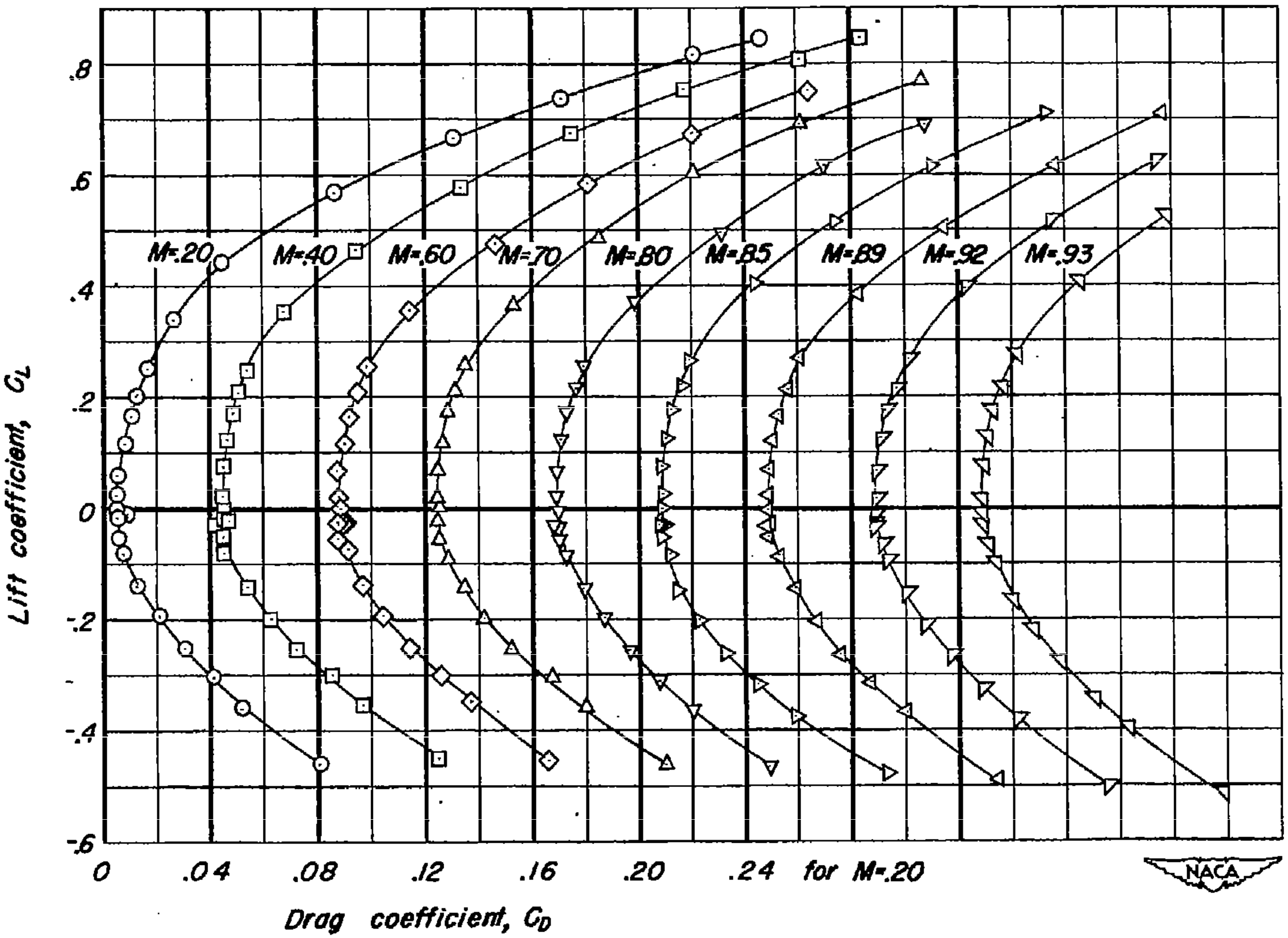

(a) C_L vs C_D.

Figure 5.– The effect of Mach number on the aerodynamic characteristics of the wing-fuselage combination at a Reynolds number of 2,000,000.

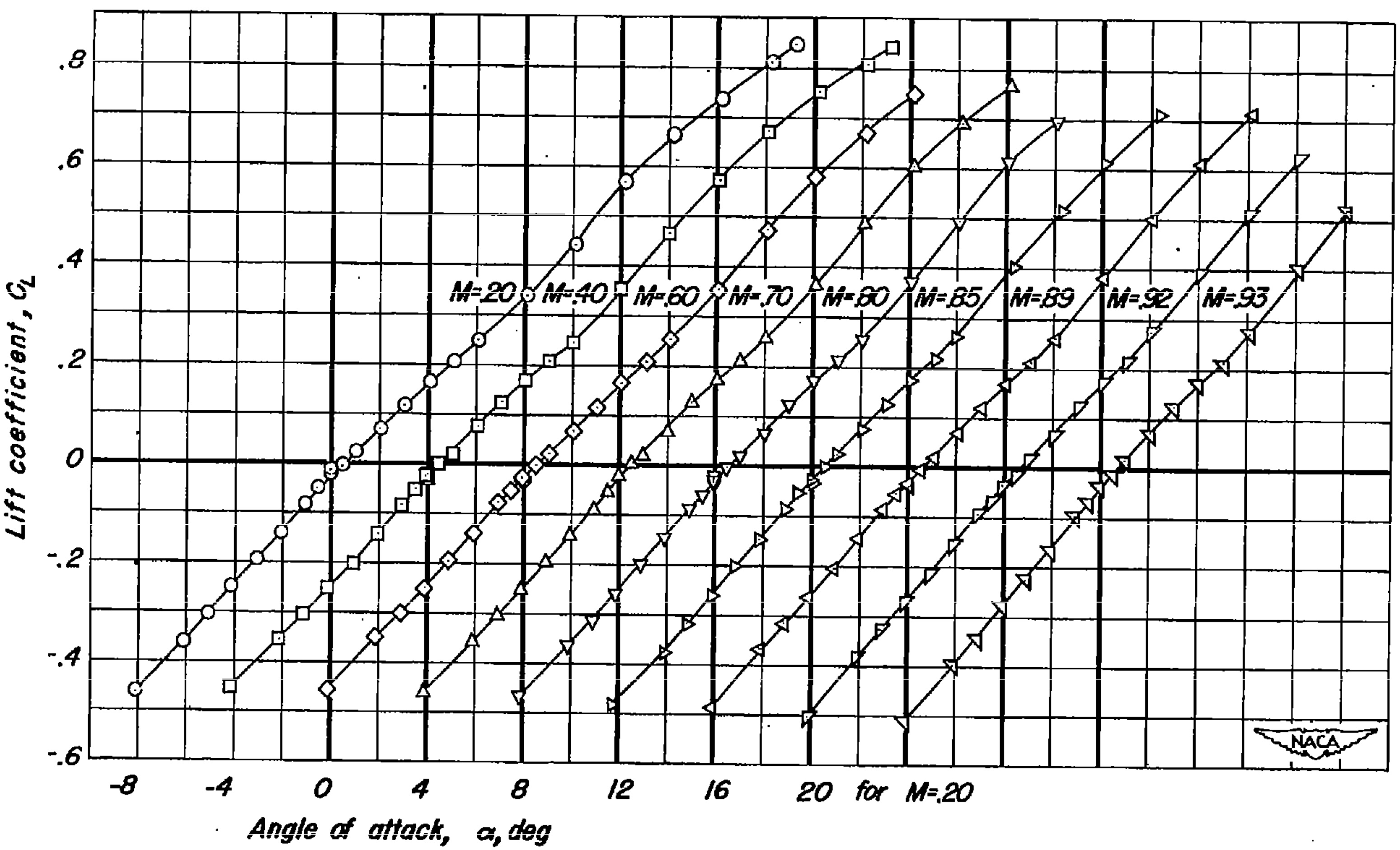

(b) C_L vs α.

Figure 5.- Continued.

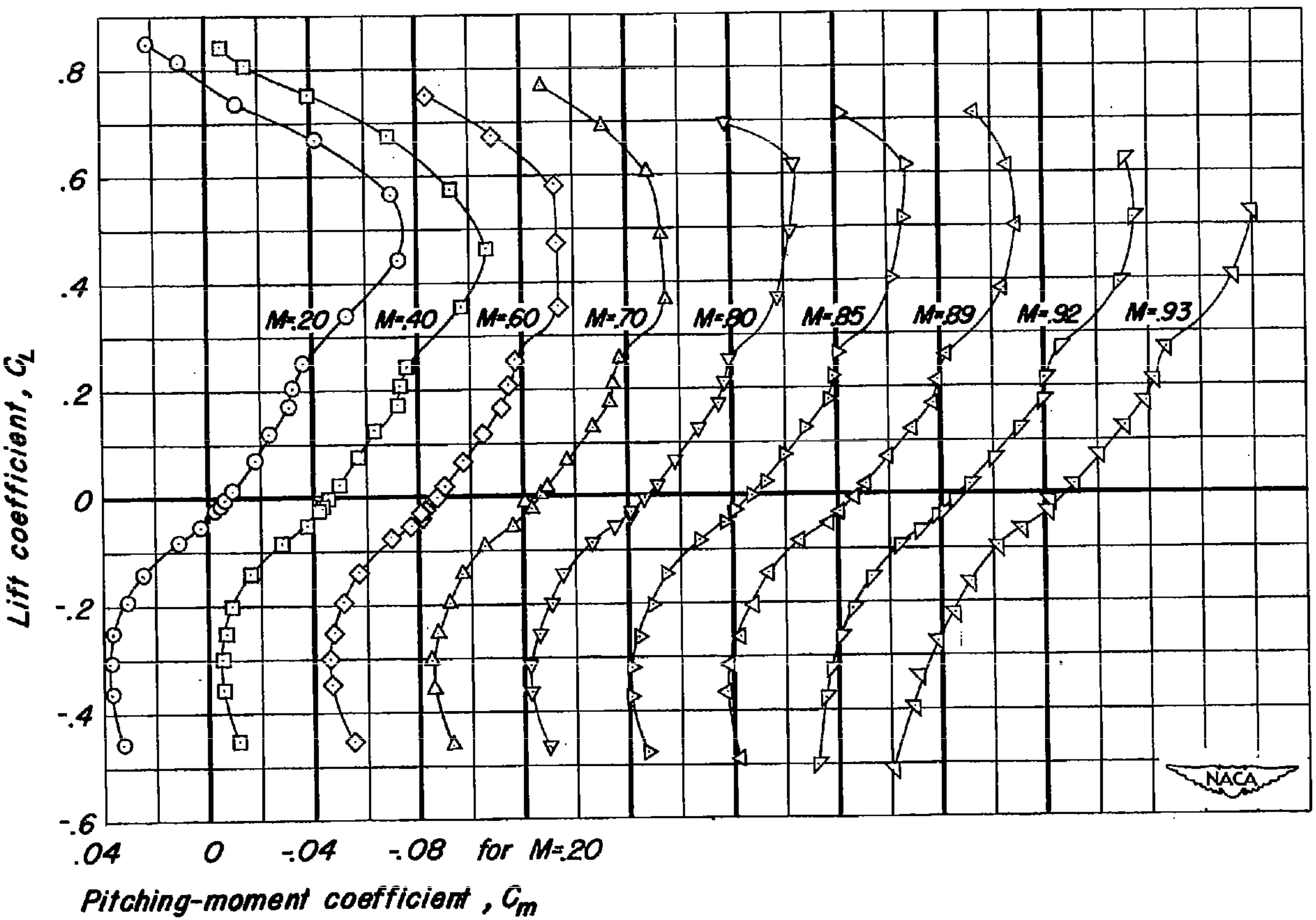

(c) C_L vs C_m.

Figure 5.– Concluded.

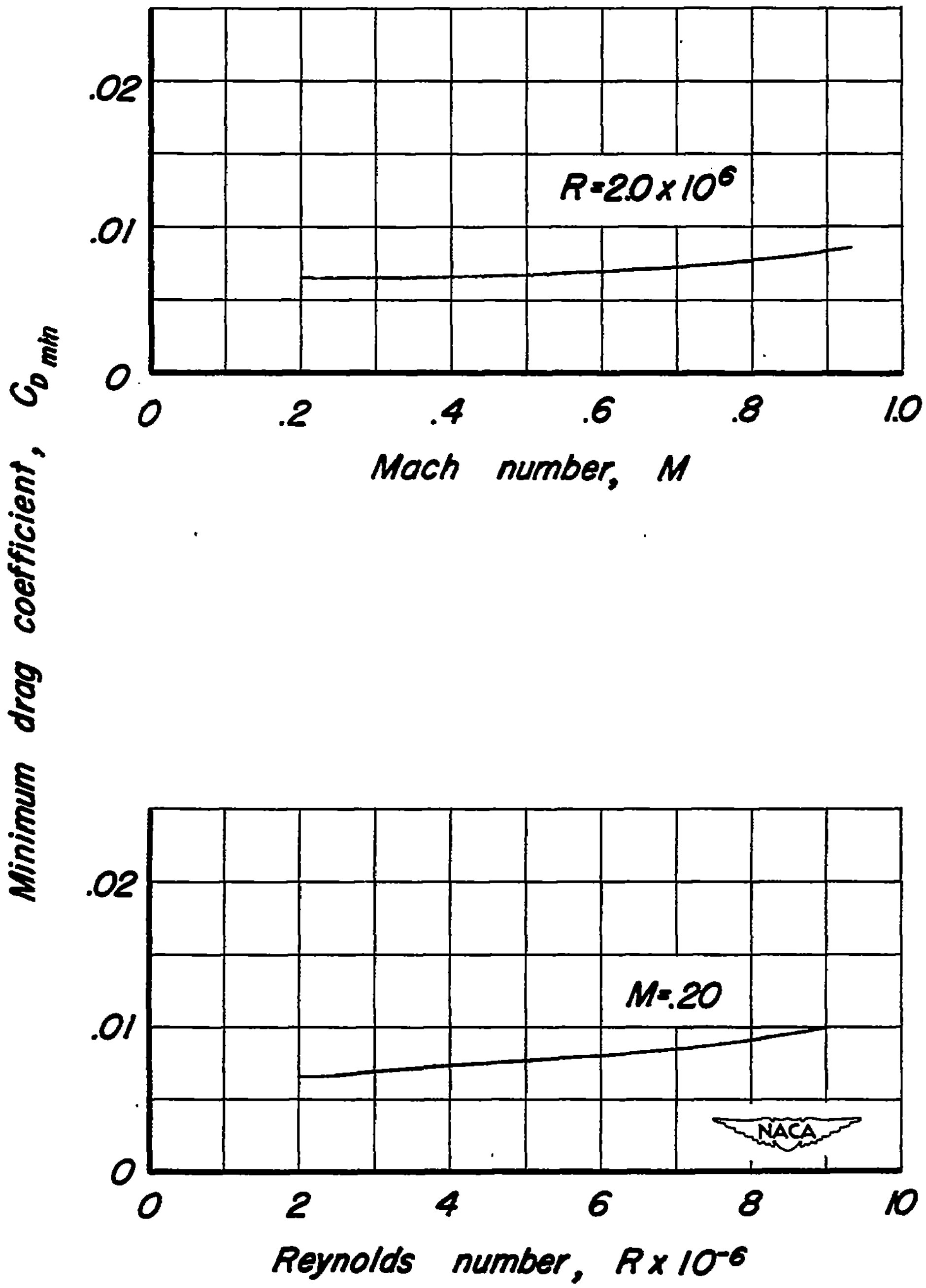

Figure 6.– The variation of the minimum drag coefficient of the wing-fuselage combination with Mach number and Reynolds number.

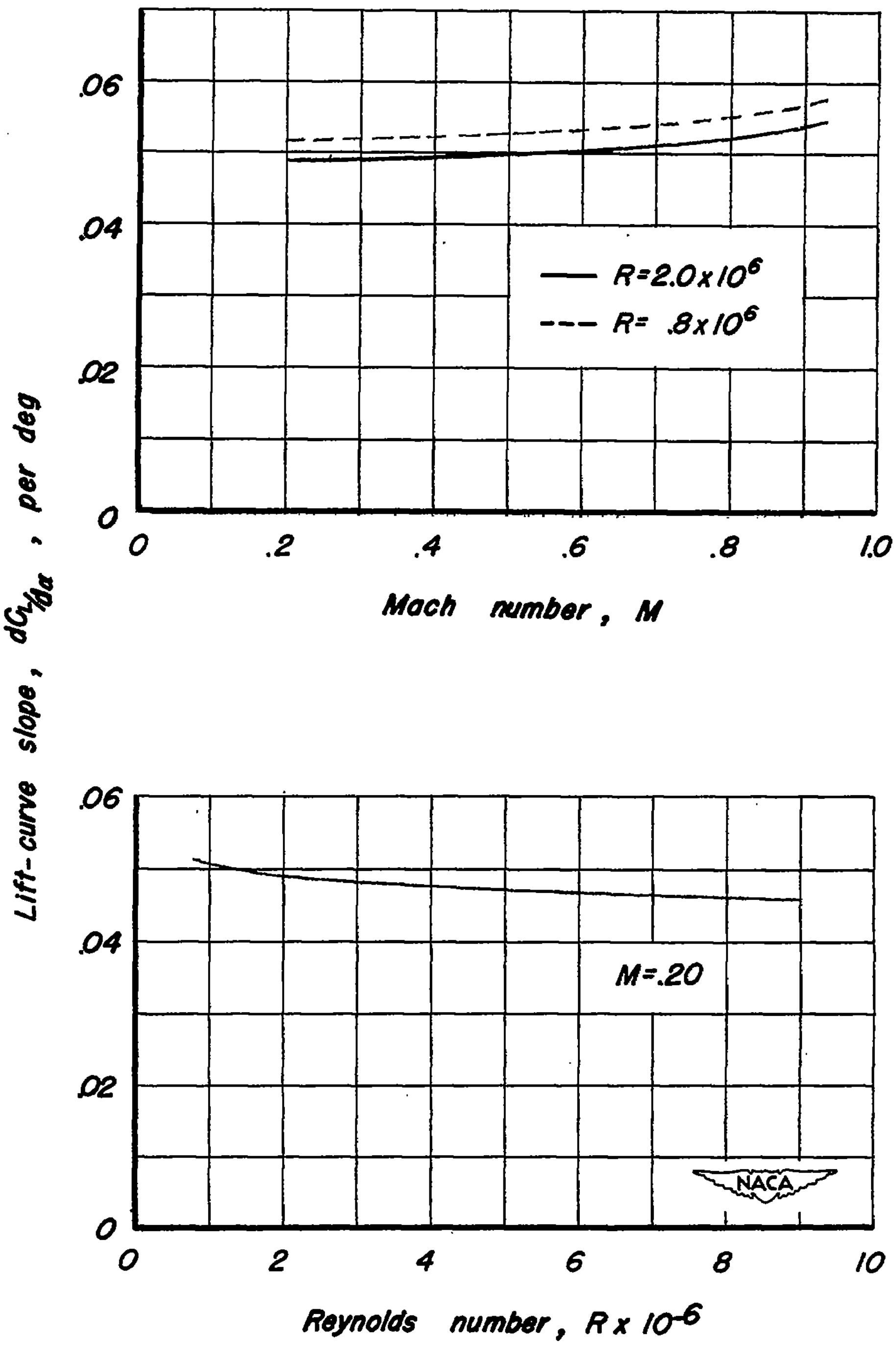

Figure 7.— The variation of lift-curve slope of the wing-fuselage combination with Mach number and Reynolds number.

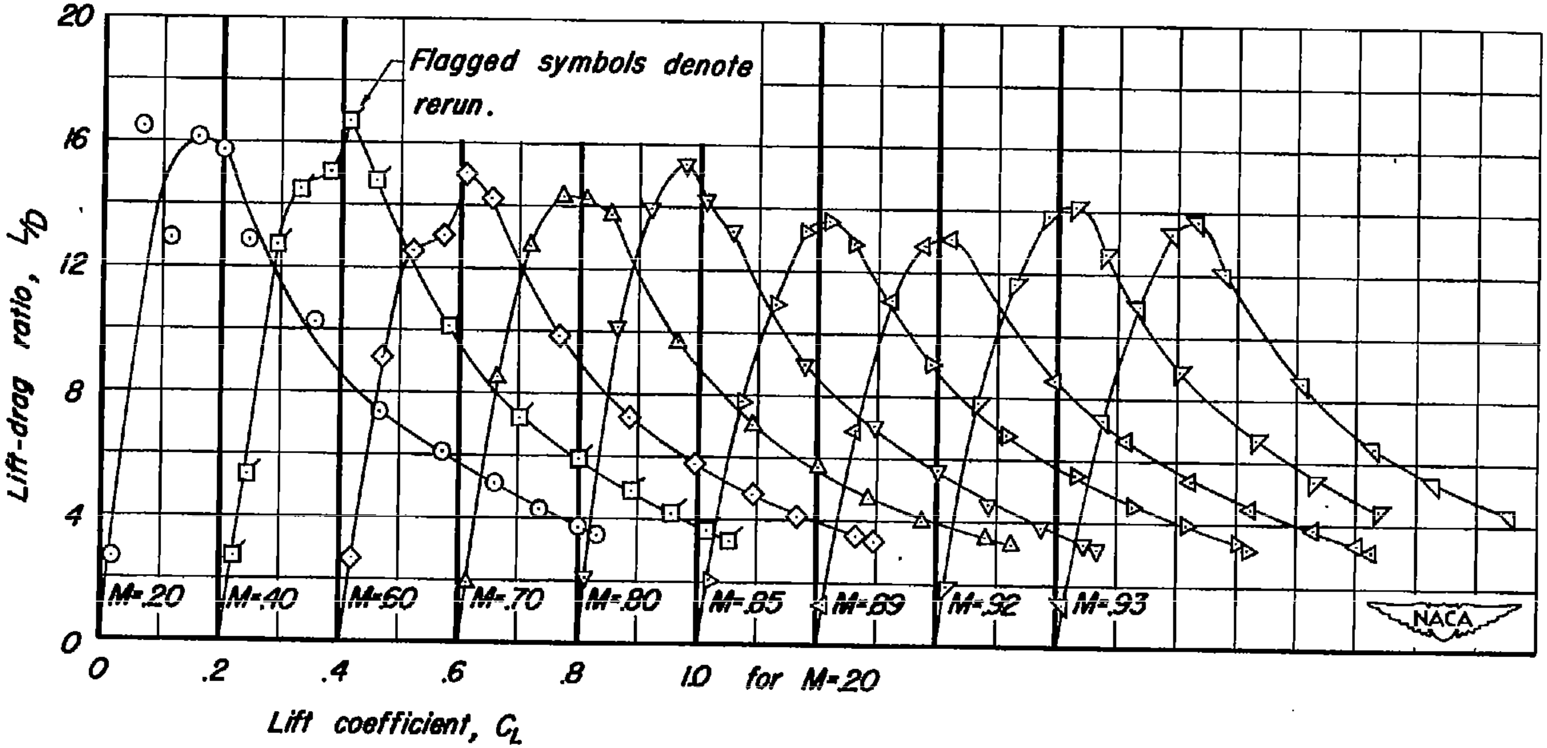

Figure 8.– The variation of lift-drag ratio with lift coefficient of the wing-fuselage combination for several Mach numbers at a Reynolds number of 800,000.

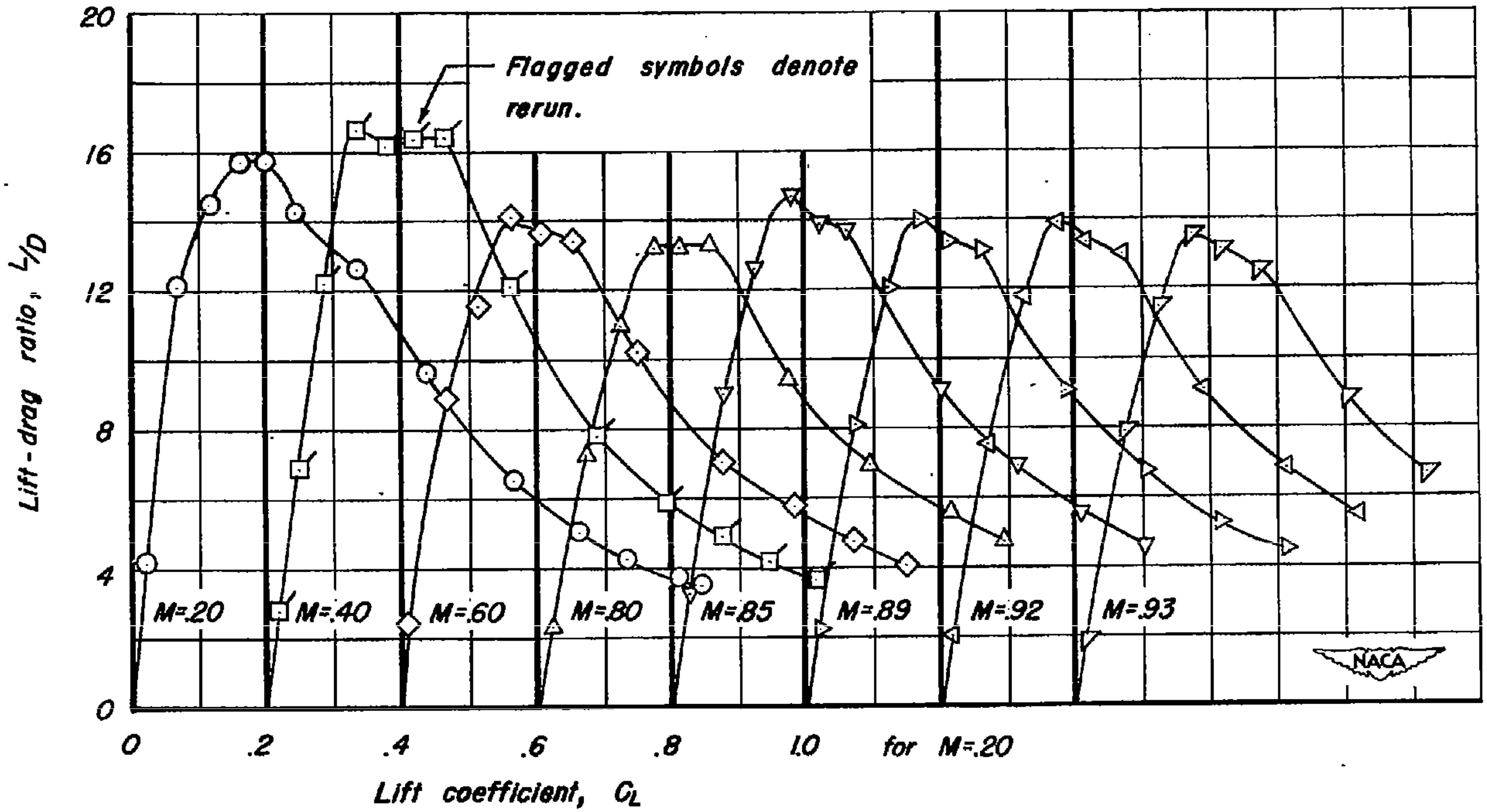

Figure 9.– The variation of lift-drag ratio with lift coefficient of the wing-fuselage combination for several Mach numbers at a Reynolds number of 2,000,000.

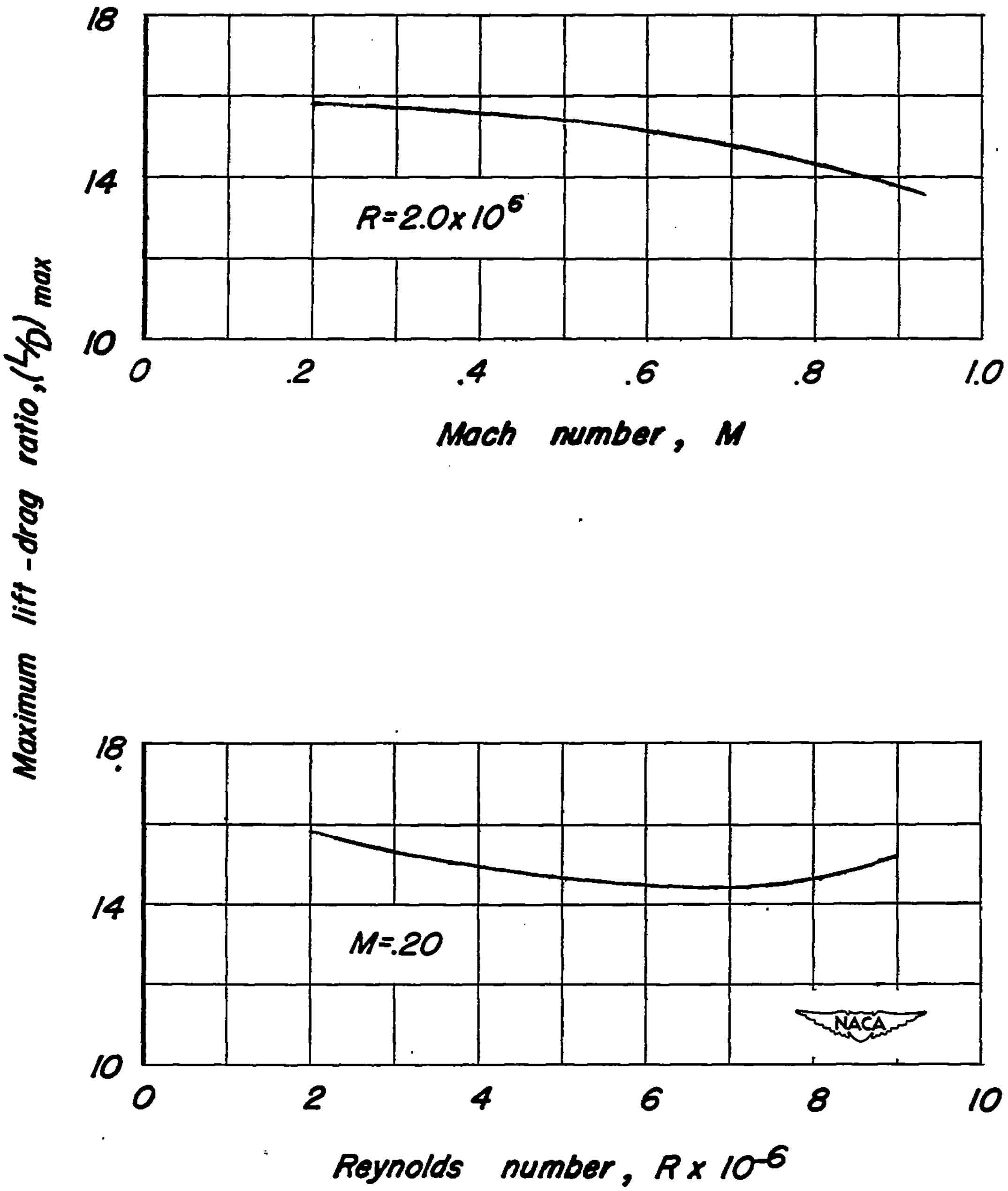

Figure 10.— The variation of the maximum lift-drag ratio of the wing-fuselage combination with Mach number and Reynolds number.

[redacted]

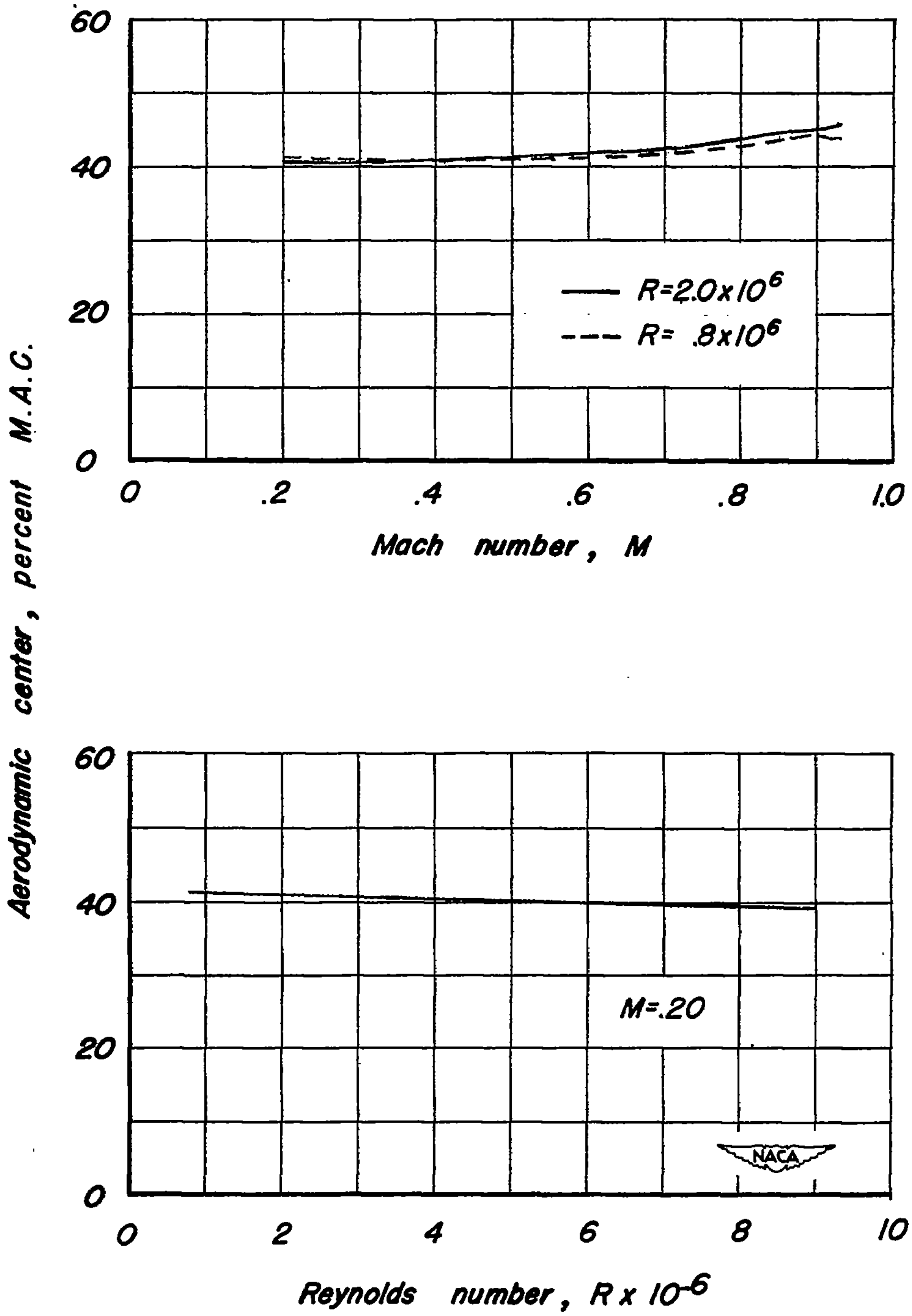

Figure 11.– The variation of the aerodynamic center (C_L=0) of the wing-fuselage combination with Mach number and Reynolds number.

[redacted]

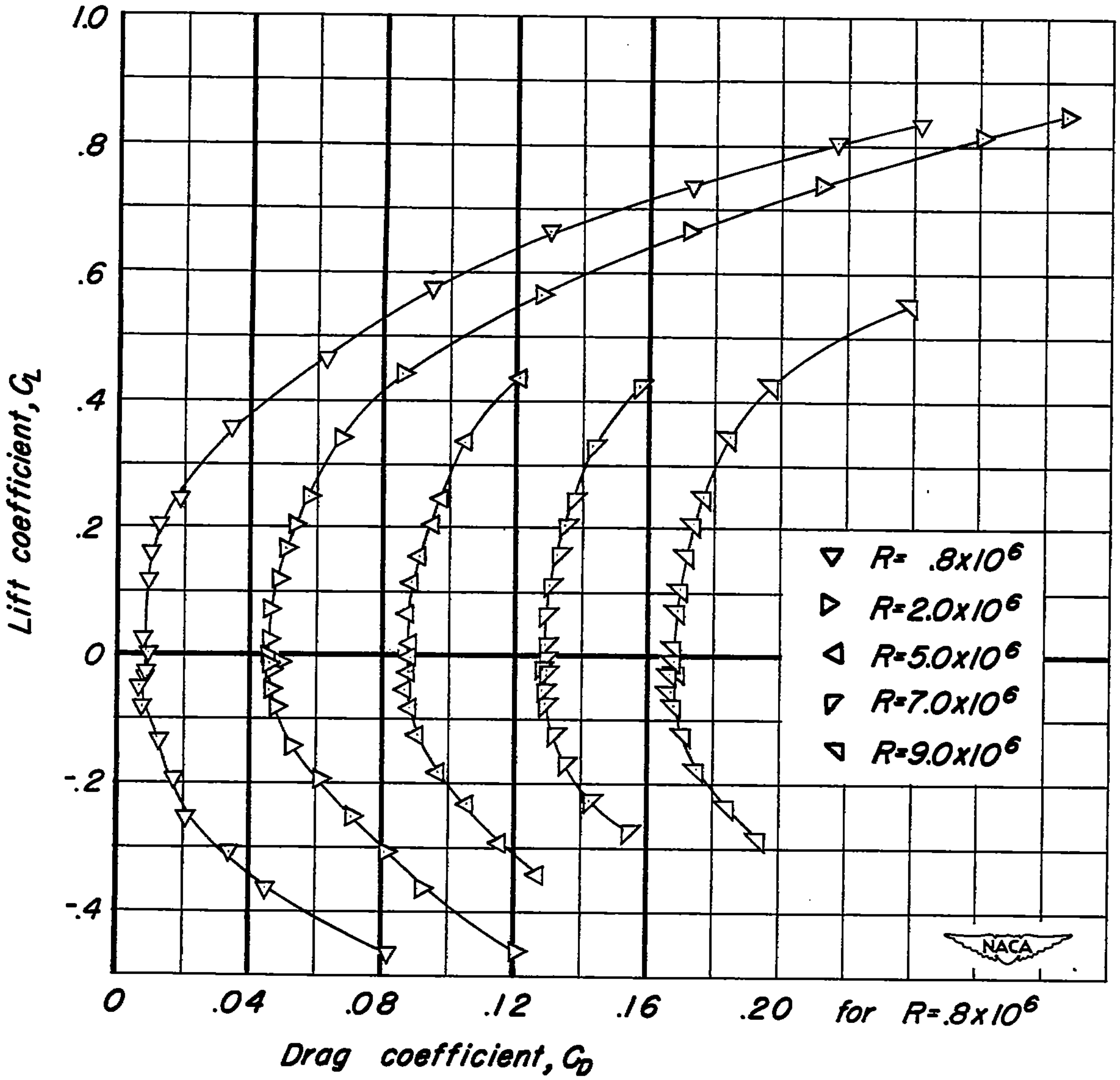

(a) C_L vs C_D.

Figure 12.- The effect of Reynolds number on the aerodynamic characteristics of the wing-fuselage combination at a Mach number of 0.20.

[redacted]

CONFIDENTIAL

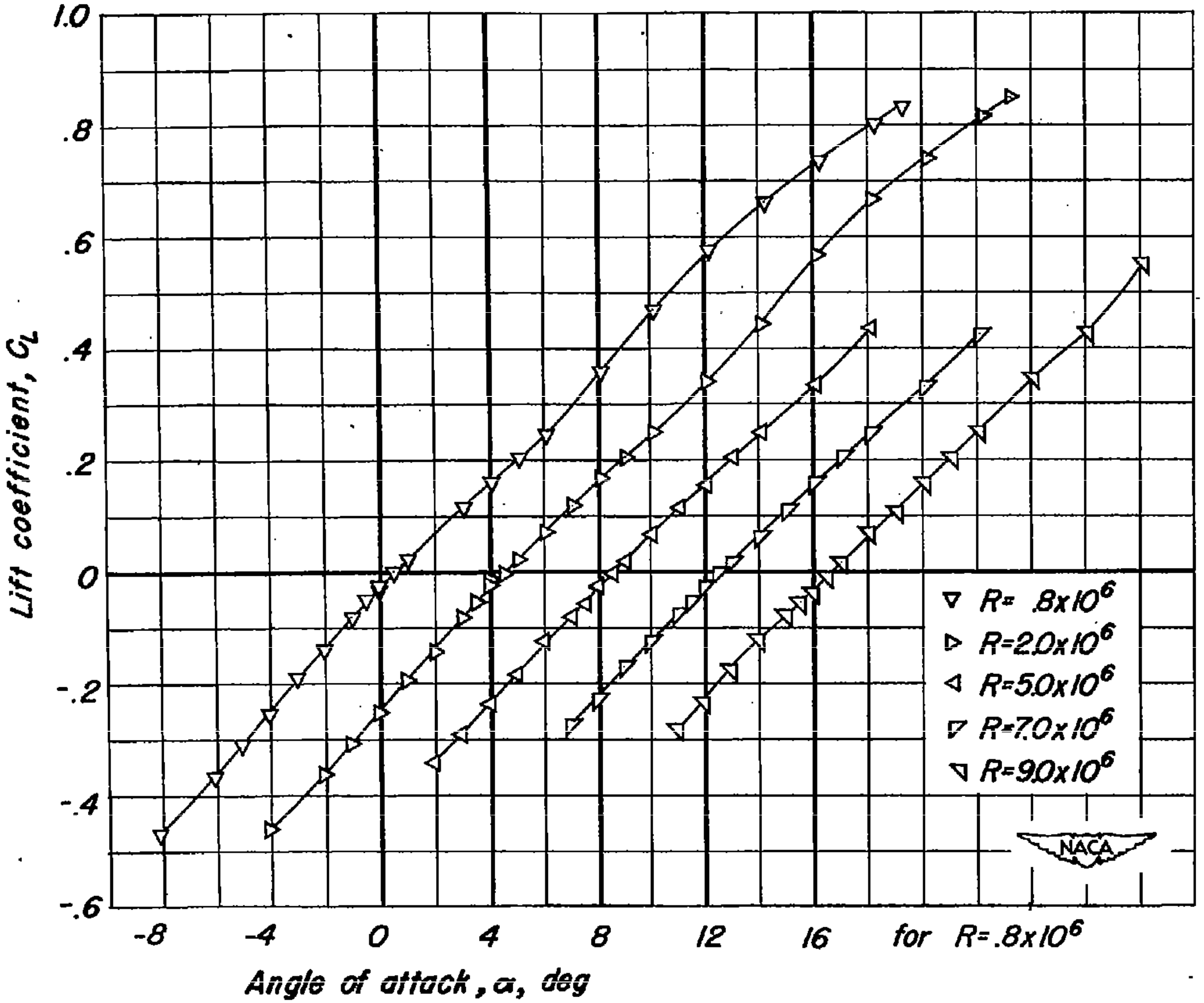

(b) C_L vs α.

Figure 12.- Continued.

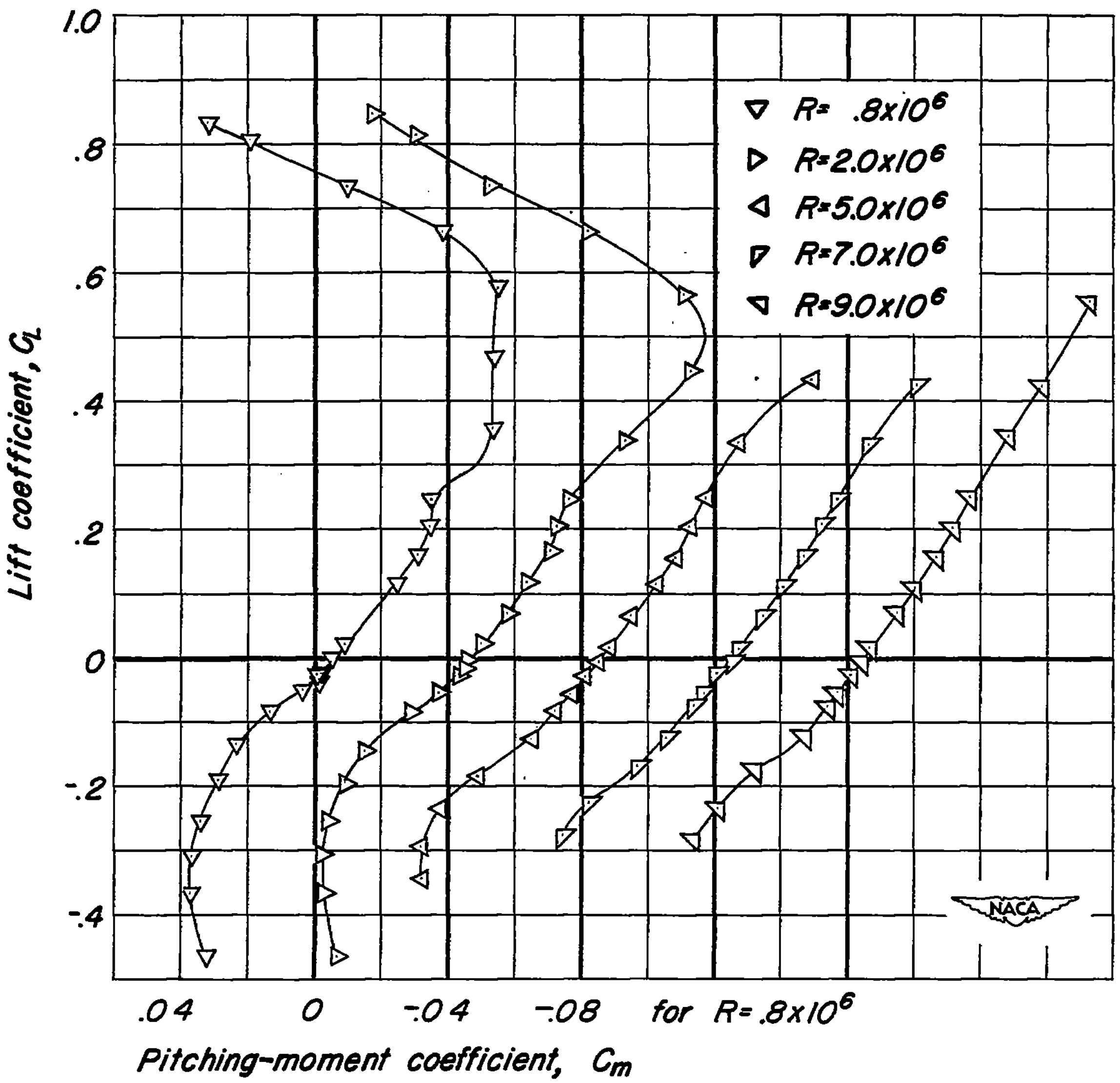

(c) C_L vs C_m

Figure 12.- Concluded.

[redacted]

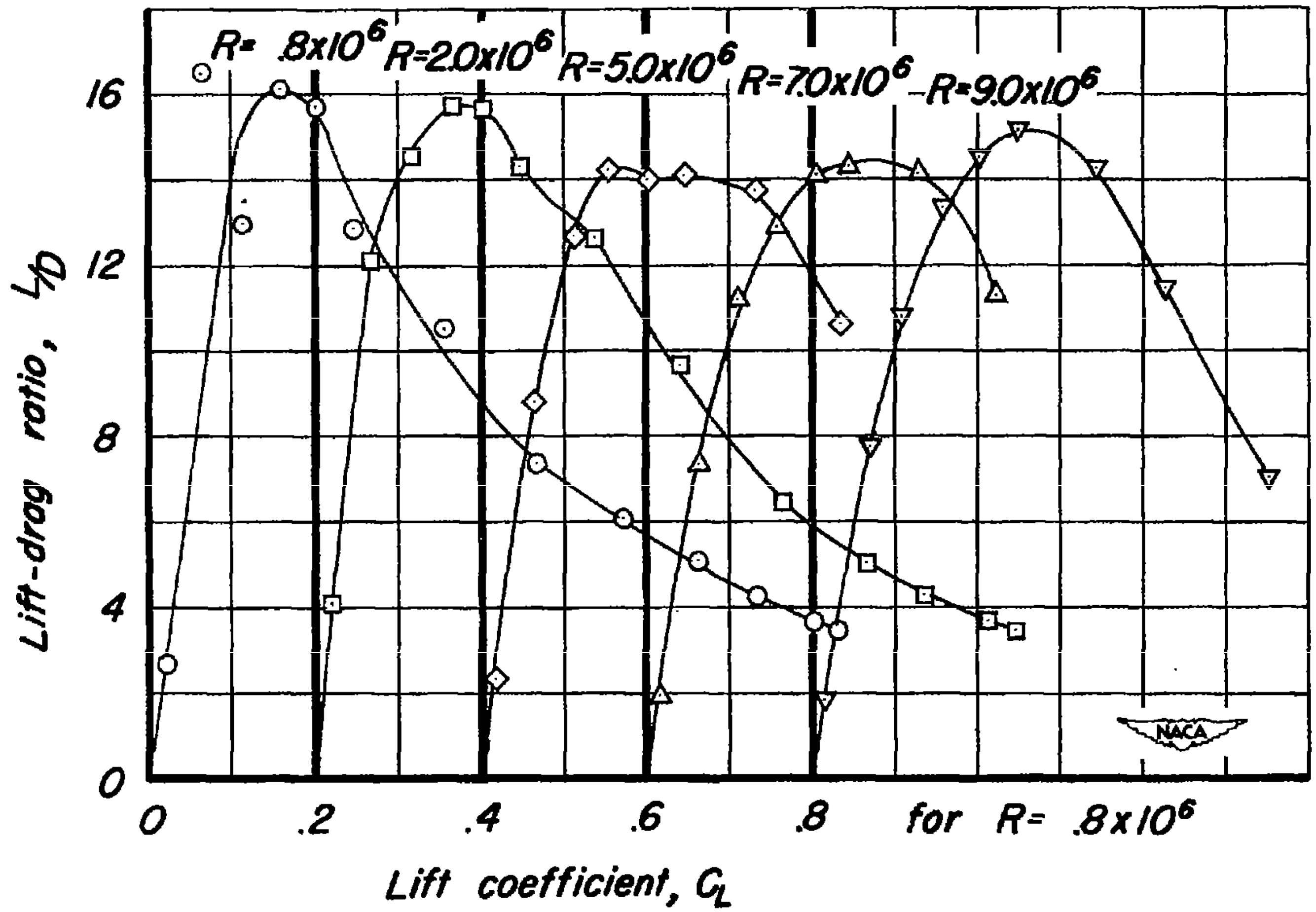

Figure 13.– The variation of lift-drag ratio with lift coefficient of the wing-fuselage combination at several Reynolds numbers at a Mach number of 0.20.

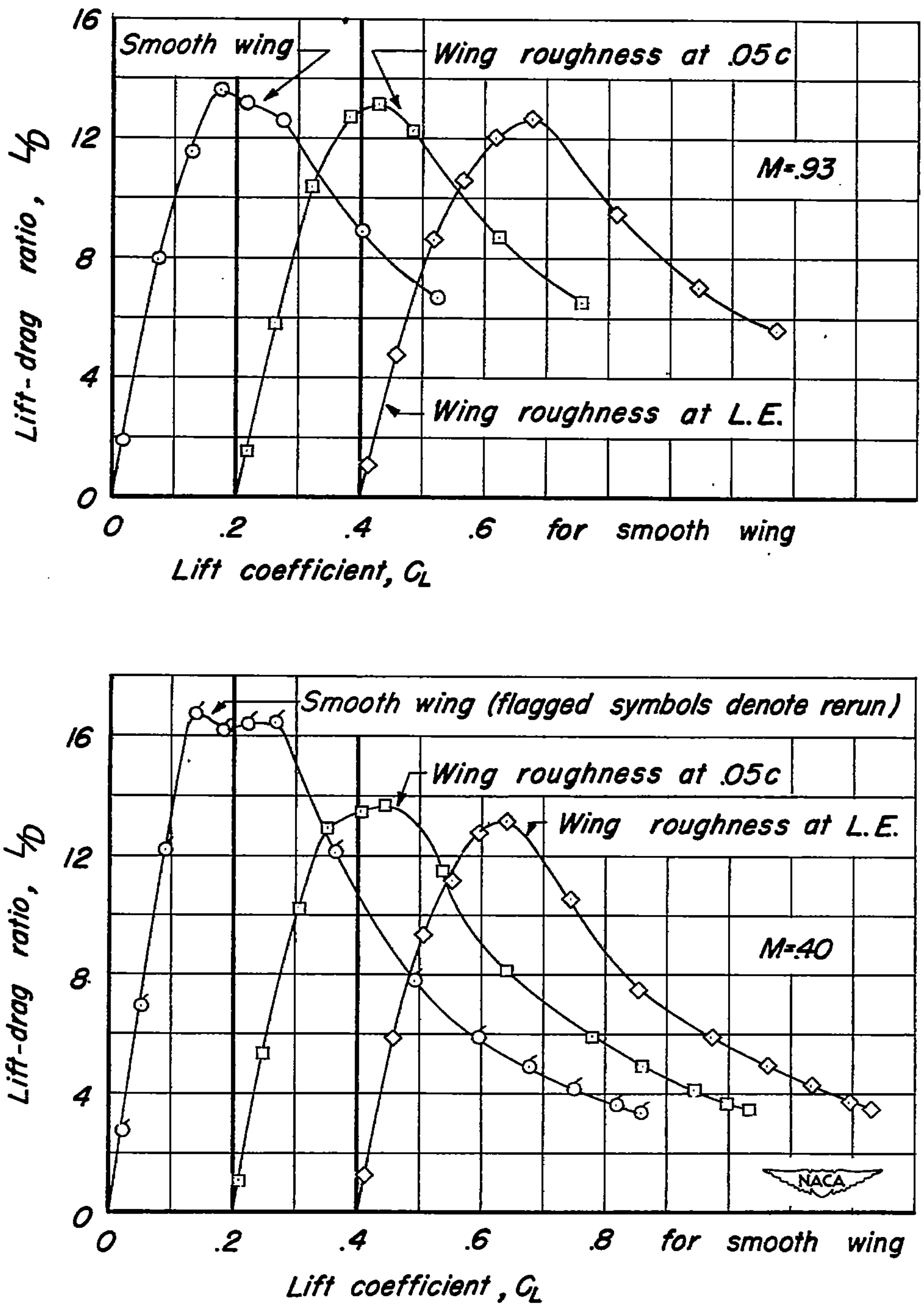

Figure 14.–The effects of wing roughness on the variation of lift-drag ratio with lift coefficient of the wing-fuselage combination at a Reynolds number of 2,000,000.

[redacted]

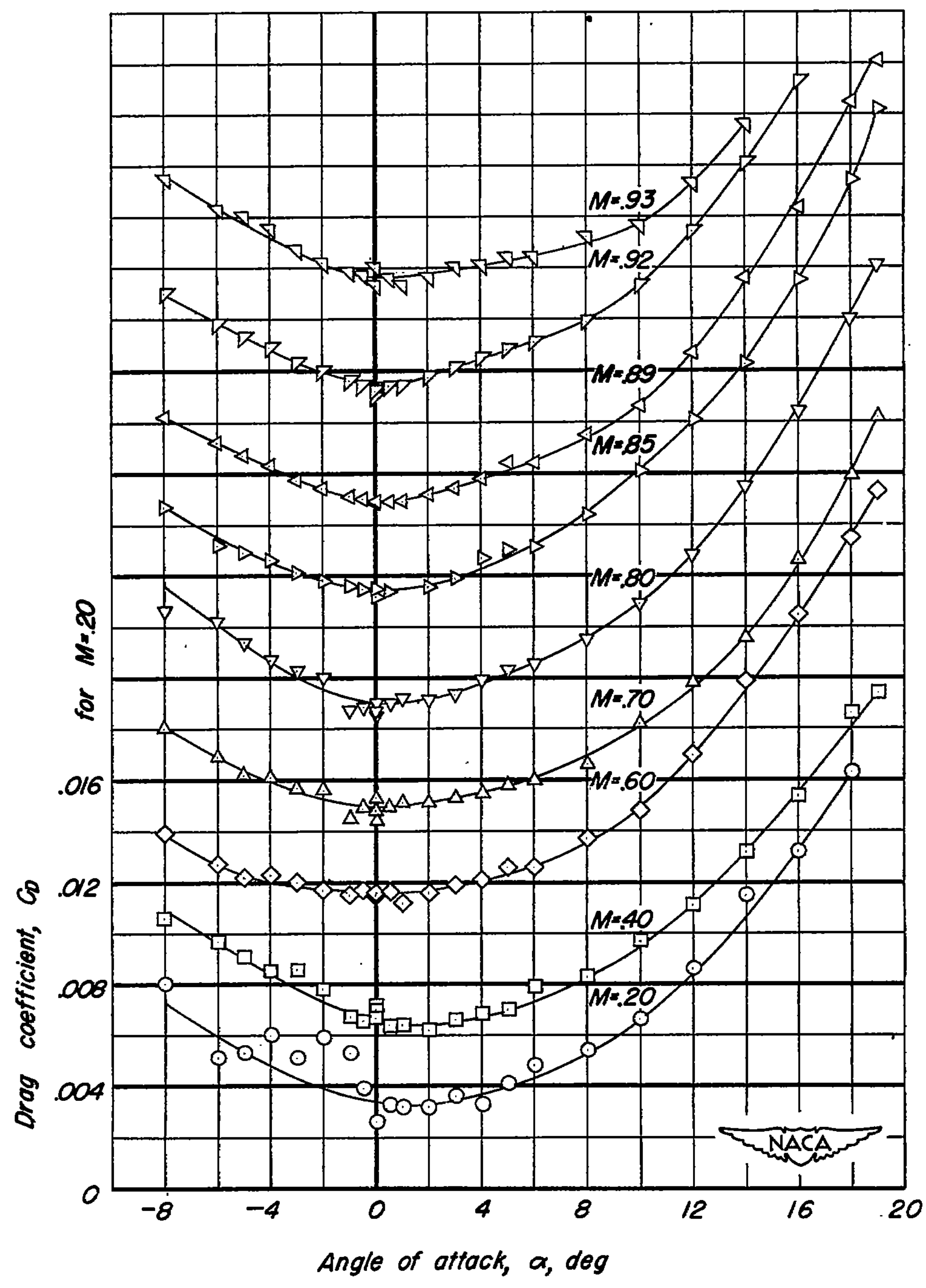

(a) C_D vs α.

Figure 15.- The effect of Mach number on the aerodynamic characteristics of the fuselage at a Reynolds number of 2,000,000.

[redacted]

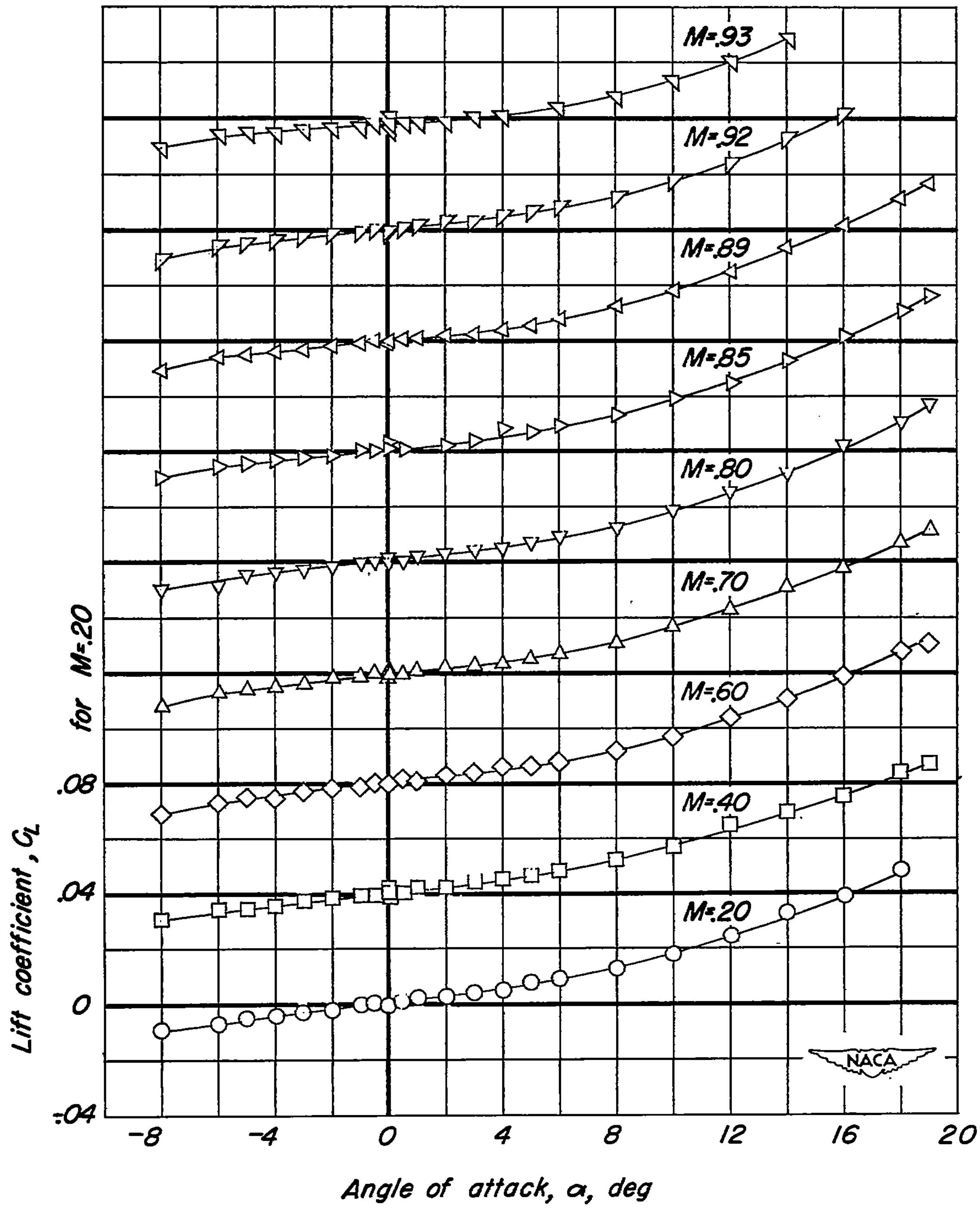

(b) C_L vs α.

Figure 15.- Continued.

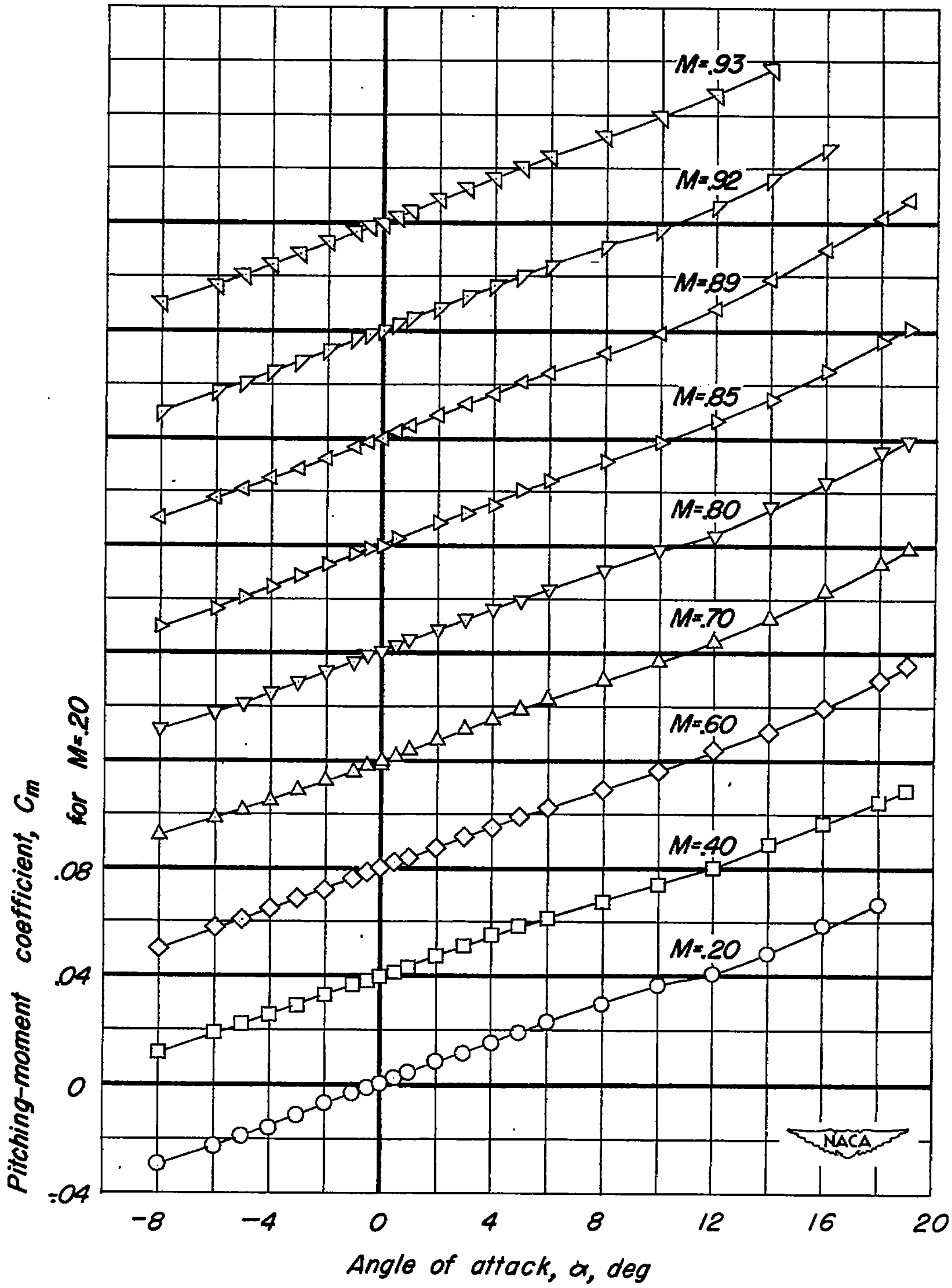

(c) C_m vs α.

Figure 15.- Concluded.

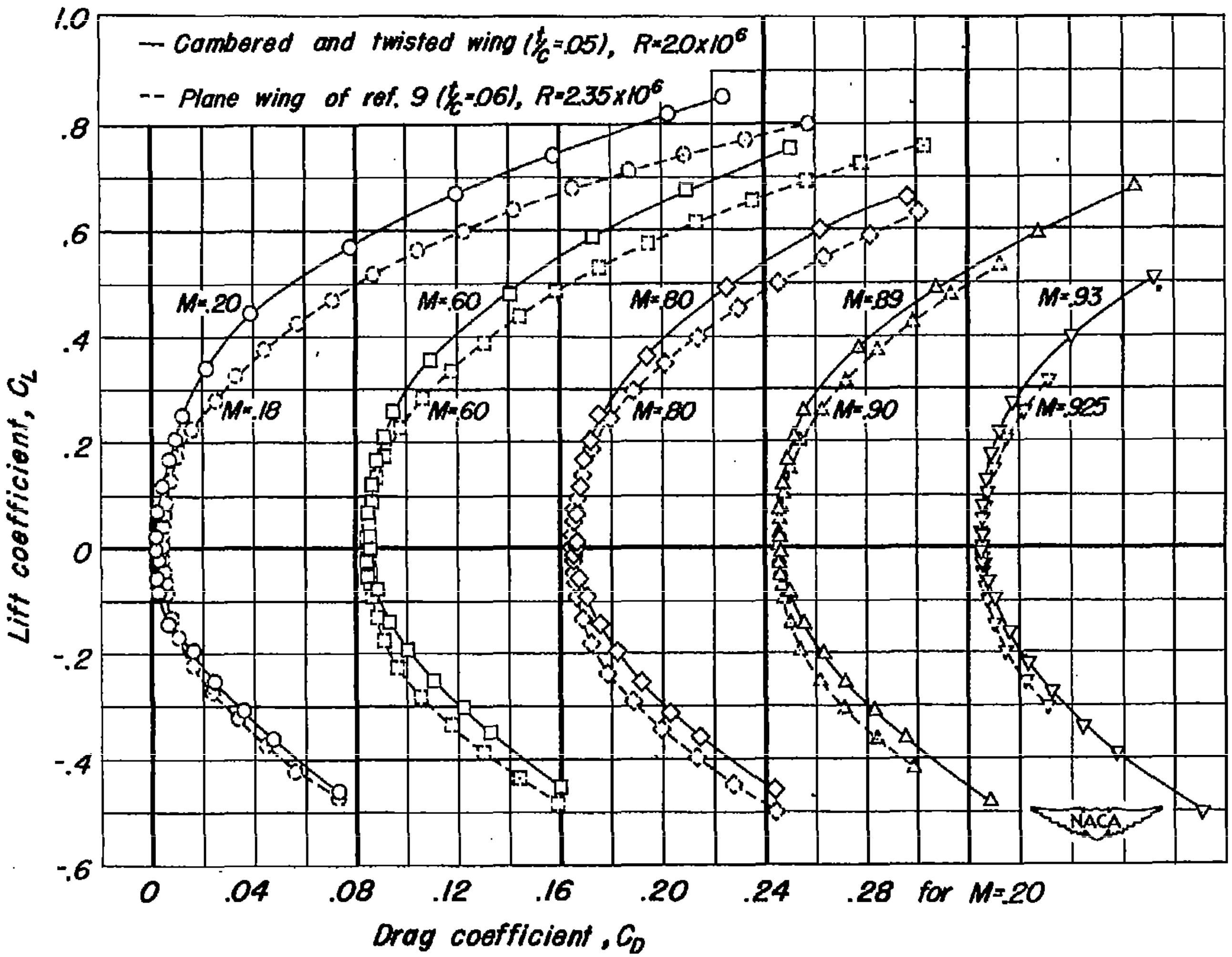

(a) C_L vs C_D.

Figure 16.- Aerodynamic characteristics at several Mach numbers of the cambered and twisted wing and of a wing of identical plan form having no camber or twist.

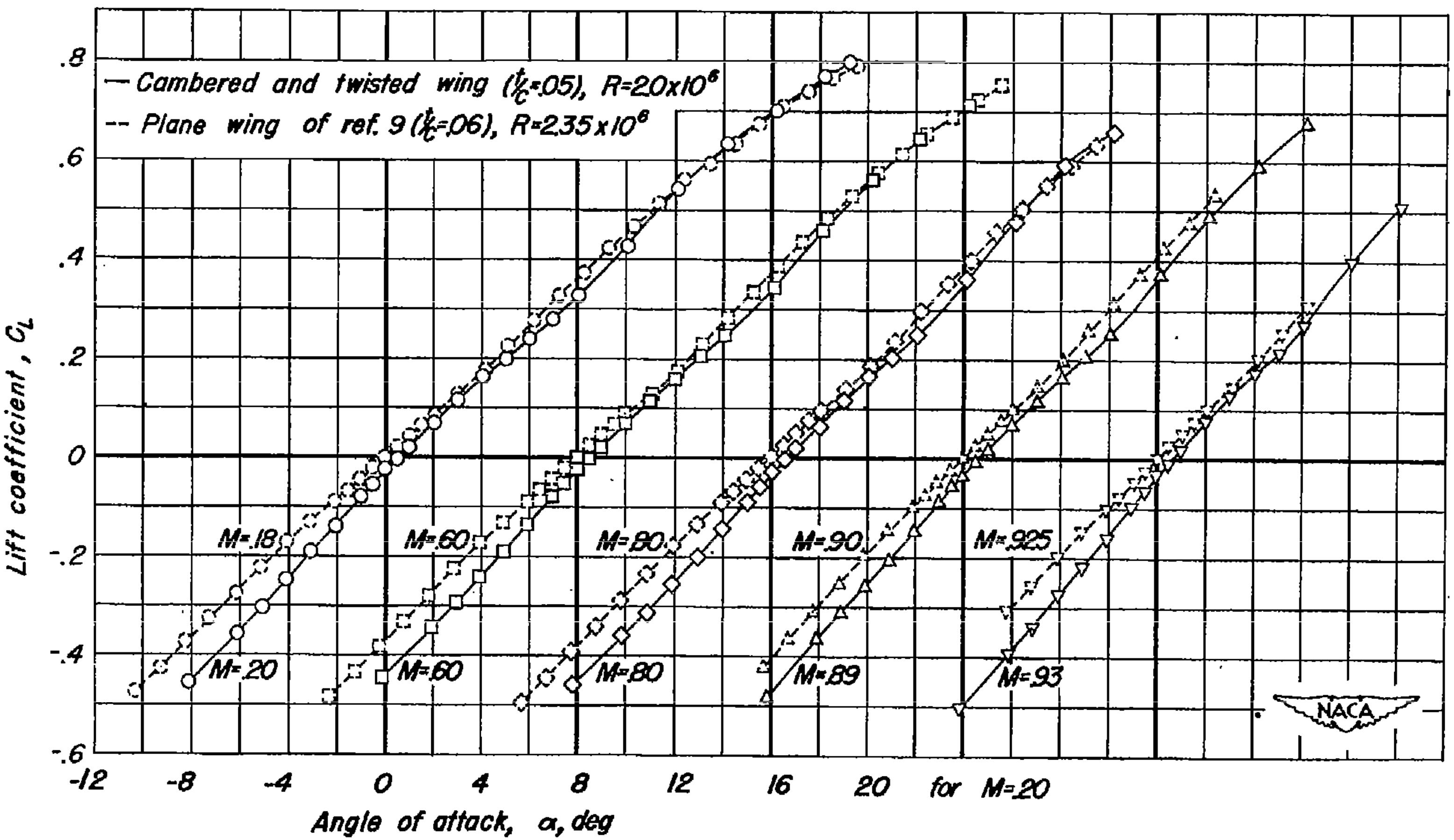

(b) C_L vs α.

Figure 16.– Continued.

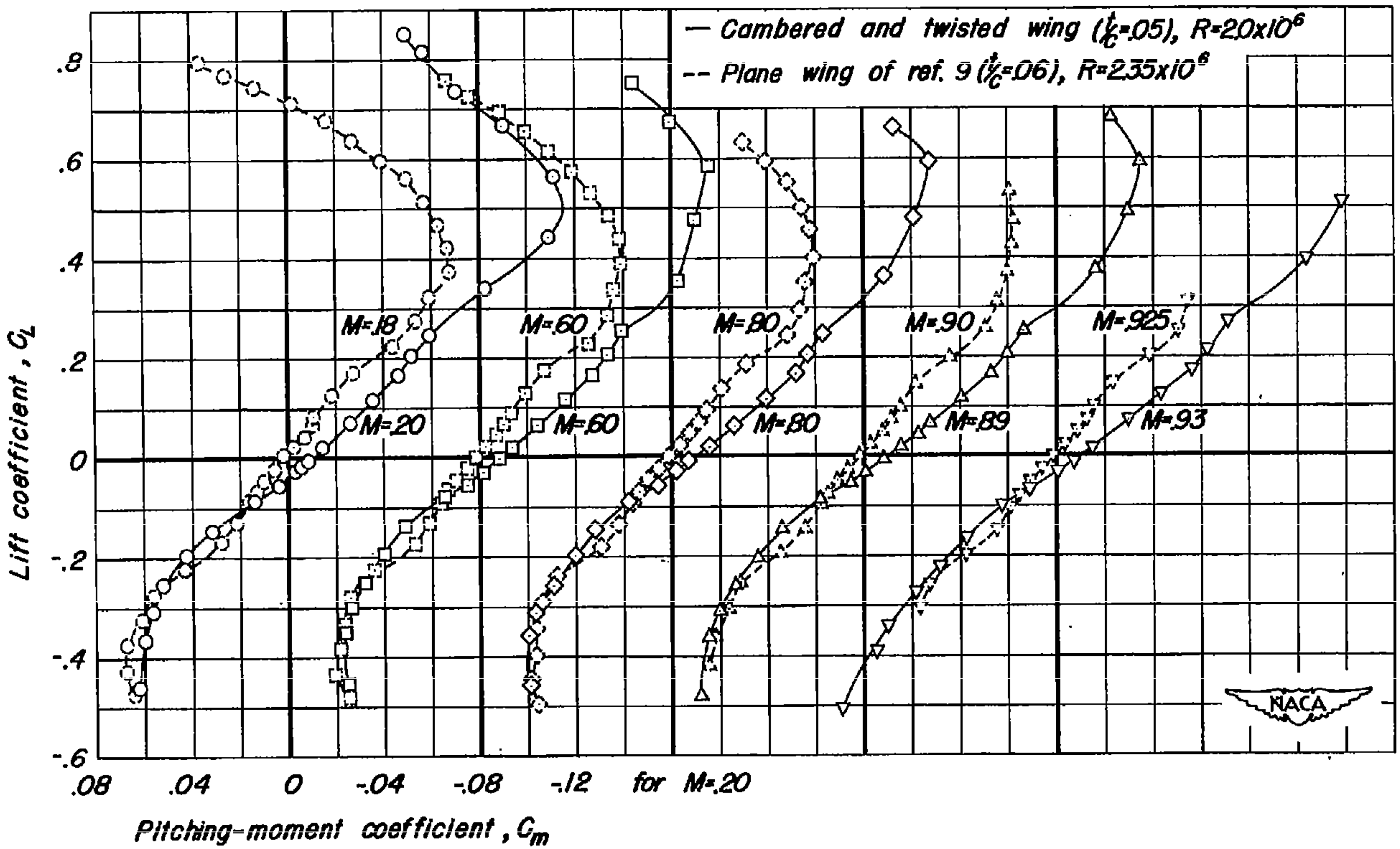

(c) C_L vs C_m.

Figure 16.- Concluded.